Applied Mathematics and Computation 462 (2024) 128330

Contents lists available at ScienceDirect

Applied Mathematics and Computation

journal homepage: www.elsevier.com/locate/amc

A local simplex spline basis for C^3 quartic splines on arbitrary triangulations

Tom Lyche [a], Carla Manni [b], Hendrik Speleers [b,*]

[a] Department of Mathematics, University of Oslo, Norway
[b] Department of Mathematics, University of Rome Tor Vergata, Italy

ARTICLE INFO

Keywords:
C^3 quartic splines
B-splines
Simplex splines
Wang–Shi macro-structure
Triangulations

ABSTRACT

We deal with the problem of constructing, representing, and manipulating C^3 quartic splines on a given arbitrary triangulation $\mathcal{T}$, where every triangle of $\mathcal{T}$ is equipped with the quartic Wang–Shi macro-structure. The resulting C^3 quartic spline space has a stable dimension and any function in the space can be locally built via Hermite interpolation on each of the macro-triangles separately, without any geometrical restriction on $\mathcal{T}$. We provide a simplex spline basis for the space of C^3 quartics defined on a single macro-triangle which behaves like a B-spline basis within the triangle and like a Bernstein basis for imposing smoothness across the edges of the triangle. The basis functions form a nonnegative partition of unity, inherit recurrence relations and differentiation formulas from the simplex spline construction, and enjoy a Marsden-like identity.

1. Introduction

Splines, in the classical sense of the term, are piecewise functions consisting of polynomial pieces glued together in a certain smooth way, usually by imposing equality of derivatives up to a given order. Besides their theoretical interest, splines find application in a wide range of contexts such as geometric modeling, signal processing, data analysis, visualization, and numerical simulation, just to mention a few. For many of these applications, a high smooth join between the different pieces is beneficial or even required [6,13].

In the univariate case, splines of maximal smoothness, i.e., piecewise polynomials of degree d with C^{d-1} joins, are the most popular splines. In fact, smoother splines give the same approximation order as less smooth splines of the same degree but involve fewer degrees of freedom and have less tendency to oscillate [14,24].

When moving to the bivariate setting and considering polygonal partitions, e.g., triangulations, maximal smoothness is still very appealing but becomes an arduous task to achieve. Bivariate spline spaces with too low degree compared to the smoothness are exposed to several shortcomings: they may lack a stable dimension, optimal approximation power, and stable locally supported bases. In addition, the practical wish of constructing any function of the spline space locally on each of the elements of the partition

* Corresponding author.
E-mail addresses: tom@math.uio.no (T. Lyche), manni@mat.uniroma2.it (C. Manni), speleers@mat.uniroma2.it (H. Speleers).

https://doi.org/10.1016/j.amc.2023.128330

Available online 20 September 2023

($\mathcal{T}$) may require a significant gap between the degree (d) and the smoothness (r). For instance, on a triangulation a degree $d \geq 4r+1$ is necessary to admit such a local construction [3,13,33].

The above drawbacks can be mitigated by considering a so-called *macro-structure*, where the partition $\mathcal{T}$ is further refined in a specific manner (often referred to as *splits*). In case $\mathcal{T}$ is a triangulation, the most famous examples are the Clough–Tocher (CT) split [3,4,13,23] and the Powell–Sabin (PS) 6 and 12 splits [1,13,21,23,25]. They subdivide each triangle of $\mathcal{T}$ into 3, 6, and 12 subtriangles, respectively. Nevertheless, no spline spaces of maximal smoothness $r = d-1$ can be constructed over general triangulations with the above mentioned splits for degree $d > 2$; see, e.g., [13].

In [32], Wang and Shi introduced a family of degree-dependent splitting schemes to refine any triangle Δ of a given triangulation. The split of degree d is obtained by uniformly distributing $d+1$ points on each edge of Δ and by taking the complete graph connecting these boundary points. For $d = 1$ we have no split and for $d = 2$ the Wang–Shi (WS) split reduces to the PS-12 split. Contrarily to the well-known splits mentioned above, when d increases, the family of WS splits generates a very large number of polygonal pieces in each Δ. For cubics we get a set of 75 polygons which includes triangles, quadrilaterals, and pentagons, while for quartics the split consists of 250 polygonal regions. Thanks to this very articulated geometry, the cubic/quartic WS splits allow us to locally construct C^2 cubic/C^3 quartic spline spaces on general triangulations. Unfortunately, in practice, the complexity of the geometry hampers a piecewise treatment — in terms of a local polynomial basis — of spline functions on WS splits and discourages the use of such interesting spaces.

To overcome this issue, a simplex spline basis for the local space of C^2 cubics on the cubic WS split of any Δ in $\mathcal{T}$ has been presented in [15]. Such a basis behaves like a B-spline basis within each triangle of $\mathcal{T}$ and like a Bernstein basis for imposing smoothness across the edges of $\mathcal{T}$. More precisely, the basis functions form a nonnegative partition of unity, inherit recurrence relations and differentiation formulas from the simplex spline structure, and enjoy a Marsden-like identity for the representation of cubic polynomials. Moreover, they admit simple conditions for C^2 joins to neighboring triangles in $\mathcal{T}$ and a control net can be set up that mimics the shape of the spline function. Other simplex spline bases for local spline spaces over a macro-triangle have been considered for the PS-12 split in [5,19] and for the CT split in [16,18]. The multivariate Alfeld split has been addressed in [17].

In this paper, we consider the quartic WS split for constructing C^3 quartic splines on a general triangulation $\mathcal{T}$. Given the complex geometry of the split, it is imperative to produce a basis for the local spline space over each (refined) triangle Δ in $\mathcal{T}$ that intrinsically avoids in its construction to deal with separate polynomial representations on each of the 250 polygonal subelements of Δ. Taking into account the complete graph structure of the WS split, a basis formed by (scaled) simplex splines emerges again as the natural solution to the problem. We construct such a basis for the local space of C^3 quartics on the quartic WS split of Δ and attain properties similar to the cubic case. The local representation in terms of the simplex spline basis makes that the complex geometry of the WS split is transparent to the user, offering a pathway for effective use of the related spline space.

We remark that for all the above mentioned splits, neither the Bernstein basis nor the simplex spline basis provides a global basis for the full spline space on (the refinement of) $\mathcal{T}$. Global B-spline bases have been developed for C^1 PS spline spaces on triangulations [7,10,11,30], for PS spline spaces with higher smoothness [8,27,29], and for C^1 CT spline spaces [9,28]. A general framework to obtain a global basis is the technique of minimal determining sets described for the local Bernstein basis in [13]. The latter technique has been exploited in [15] to produce a global basis starting from local simplex spline bases for C^2 cubic splines over triangulations refined according to the cubic WS split. Although a similar approach could be used in the quartic case as well, it seems more convenient to work directly with the local representations provided by the local simplex spline basis, rather than with the global basis for the full spline space.

The remainder of this paper is divided into four sections. In Section 2, we describe the family of WS splits and we summarize the definition and some properties of simplex splines. In Section 3, we present a local simplex spline basis for the refinement of a single triangle and discuss some of its properties. An interesting subspace containing the polynomials of degree four is also provided. The full space of C^3 quartic splines is discussed in Section 4 paying special attention to smoothness conditions across the edges of the given triangulation. We end with some concluding remarks in Section 5. Finally, the appendix aggregates data related to the presented simplex spline bases that were used in the proofs and might be useful for practical purposes as well.

Throughout the paper, we use small boldface letters for vectors. Function spaces are denoted by symbols like $\mathbb{S}$. In particular, $\mathbb{P}_d$ stands for the space of bivariate polynomials with real coefficients of total degree $\leq d$. The partial derivatives in x and y are denoted by D_x and D_y, respectively. Given a vector $\boldsymbol{u}$, the associated directional derivative is denoted by $D_{\boldsymbol{u}}$. The directional derivative in the direction of the vector from point $\boldsymbol{p}_1$ to $\boldsymbol{p}_2$ is denoted by $D_{\boldsymbol{p}_1\boldsymbol{p}_2}$.

2. Preliminaries

In this section, we collect some preliminary material about the Wang–Shi splits and simplex splines of interest in the rest of the paper.

2.1. The Wang–Shi splits

Given three noncollinear points $\boldsymbol{p}_1, \boldsymbol{p}_2, \boldsymbol{p}_3$ in $\mathbb{R}^2$, the triangle $\Delta := \langle \boldsymbol{p}_1, \boldsymbol{p}_2, \boldsymbol{p}_3 \rangle$ with vertices $\boldsymbol{p}_1, \boldsymbol{p}_2, \boldsymbol{p}_3$ will serve as our macro-triangle. Given a degree $d \in \mathbb{N}$, we divide each edge of Δ into d equal segments, respectively, resulting into $3d$ boundary points. Then, we refine Δ into a number of subelements delineated by the complete graph connecting those boundary points which consists of the three edges of the triangle and of $3d(d-1)$ interior lines. The resulting partition is called the WS_d split of Δ as it was originally proposed by Wang and Shi [32]. We denote the obtained mesh structure by Δ_{WS_d}, and the set of polygons in Δ_{WS_d} by $\mathcal{P}_d$. Note

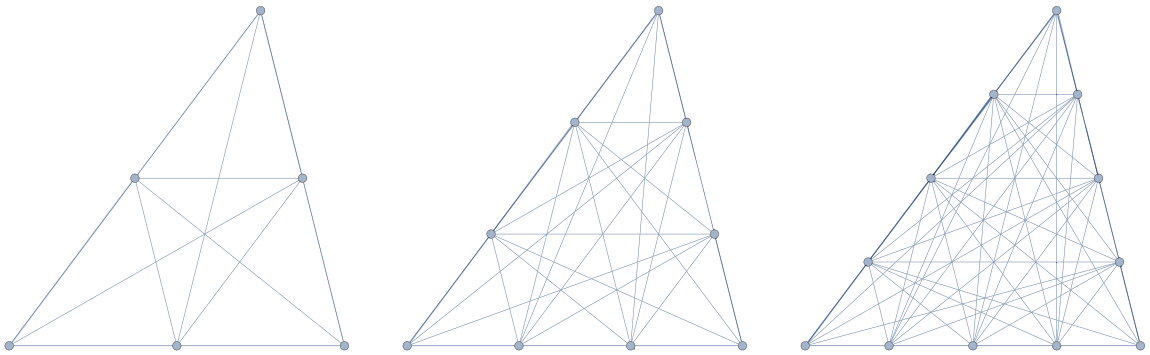

Fig. 1. WS_d splits for $d = 2, 3, 4$.

that we are dealing with a cross-cut partition of Δ because we are drawing only lines connecting boundary points. All the possible intersections of these lines are called vertices of Δ_{WS_d}. The cases $d = 2, 3, 4$ are shown in Fig. 1. For $d = 1$ we have $\mathcal{P}_1 = \{\Delta\}$, while for $d = 2$ we obtain the well-known PS-12 split [21]. For $d > 2$ not all elements of $\mathcal{P}_d$ are triangles and the complexity of the mesh grows quickly. For $d = 3$ we have 58 vertices and 75 regions, while for $d = 4$ the number of vertices increases up to 178 and we get 250 regions; see Figs. 2 and 3.

We consider the space

$$\mathbb{S}_d^{d-1}(\Delta_{\mathrm{WS}_d}) := \{ s \in C^{d-1}(\Delta) : s_{|\tau} \in \mathbb{P}_d,\ \forall\, \tau \in \mathcal{P}_d \}. \tag{1}$$

The dimension of $\mathbb{S}_d^{d-1}(\Delta_{\mathrm{WS}_d})$ can be computed using the general dimension formula for spline spaces over cross-cut partitions from [2, Theorem 3.1]. In particular, under the assumption that at most $d+1$ cross-cuts intersect at an interior vertex of Δ_{WS_d}, we have

$$\dim(\mathbb{S}_d^{d-1}(\Delta_{\mathrm{WS}_d})) = \dim \mathbb{P}_d + 3d(d-1);$$

see [15, Theorem 2]. Thus, for $d = 4$, we get

$$\dim(\mathbb{S}_4^3(\Delta_{\mathrm{WS}_4})) = \dim \mathbb{P}_4 + 36 = 51, \tag{2}$$

because it can be directly checked that at most 4 cross-cuts intersect at any interior vertex of Δ_{WS_4}; see Fig. 2.

2.2. Simplex splines

Simplex splines are a very elegant extension of univariate B-splines to the multivariate setting. Like B-splines, they are defined in terms of knots whose number and position completely determine their properties. In this section, we define simplex splines and we shortly summarize some properties of interest for the paper. For further properties and proofs, we refer the reader to, e.g., [20,22].

For $e \in \mathbb{N}$, $d \in \mathbb{N}_0$, let $n := d + e$ and let $\Xi := \{\boldsymbol{\xi}_1, \dots, \boldsymbol{\xi}_{n+1}\}$ be a sequence of possibly repeated points in $\mathbb{R}^e$ called *knots*. The multiplicity of a knot is the number of times it occurs in the sequence. For the sake of simplicity, we assume $\mathrm{vol}_e(\langle \Xi \rangle) > 0$, where $\langle \cdot \rangle$ denotes the convex hull of a sequence of points. Let $\sigma = \langle \overline{\boldsymbol{\xi}}_1, \dots, \overline{\boldsymbol{\xi}}_{n+1} \rangle$ be any simplex in $\mathbb{R}^n$ with $\mathrm{vol}_n(\sigma) > 0$, whose projection $\pi : \mathbb{R}^n \to \mathbb{R}^e$ onto the first e coordinates satisfies $\pi(\overline{\boldsymbol{\xi}}_i) = \boldsymbol{\xi}_i$ for $i = 1, \dots, n+1$.

The simplex spline M_Ξ can be defined geometrically by

$$M_\Xi : \mathbb{R}^e \to \mathbb{R}, \quad M_\Xi(\boldsymbol{x}) := \frac{\mathrm{vol}_{n-e}\left(\sigma \cap \pi^{-1}(\boldsymbol{x})\right)}{\mathrm{vol}_n(\sigma)}.$$

For $d = 0$ we have

$$M_\Xi(\boldsymbol{x}) = \begin{cases} 1/\mathrm{vol}_n(\langle \Xi \rangle), & \boldsymbol{x} \in \text{interior of } \langle \Xi \rangle, \\ 0, & \text{if } \boldsymbol{x} \notin \langle \Xi \rangle, \end{cases}$$

and the value of M_Ξ on the boundary of $\langle \Xi \rangle$ has to be dealt with separately. We refer the reader to [26] for a convention to decide in which region each edge and vertex belongs.

The simplex spline M_Ξ is a nonnegative piecewise polynomial of total degree d, supported on $\langle \Xi \rangle$ and has unit integral. Moreover, M_Ξ enjoys the following fundamental recurrence formulas, sometimes referred to as the *ABC* of simplex splines, which generalize the well-known analogs for B-splines.

- *Differentiation formula (A-recurrence)*: For any $\boldsymbol{u} \in \mathbb{R}^e$ and any $a_1, \dots, a_{d+e+1}$ such that $\sum_i a_i \boldsymbol{\xi}_i = \boldsymbol{u}$, $\sum_i a_i = 0$, we have

$$D_{\boldsymbol{u}} M_\Xi = (d+e) \sum_{i=1}^{d+e+1} a_i M_{[\Xi \setminus \boldsymbol{\xi}_i]}.$$

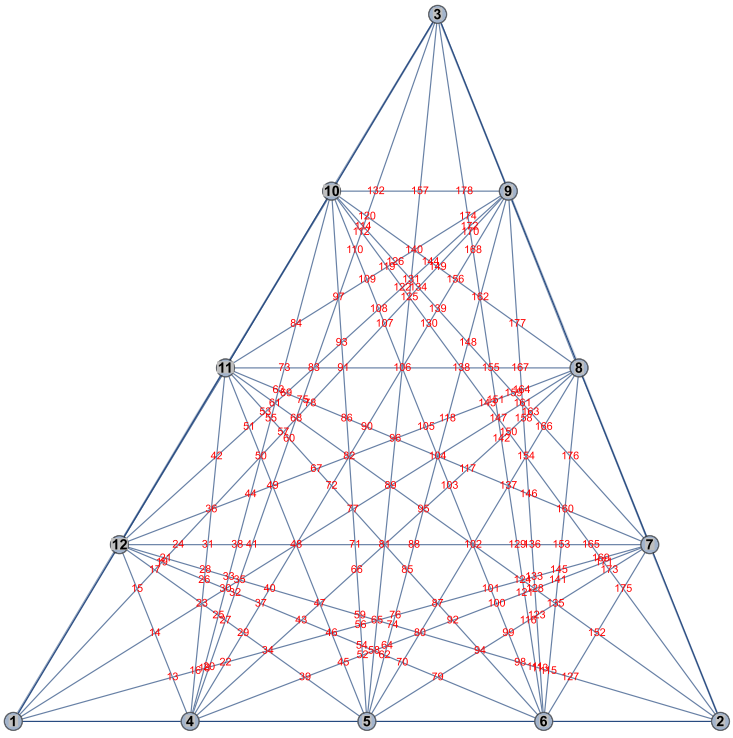

Fig. 2. A possible numbering of the 178 vertices of the WS_4 split.

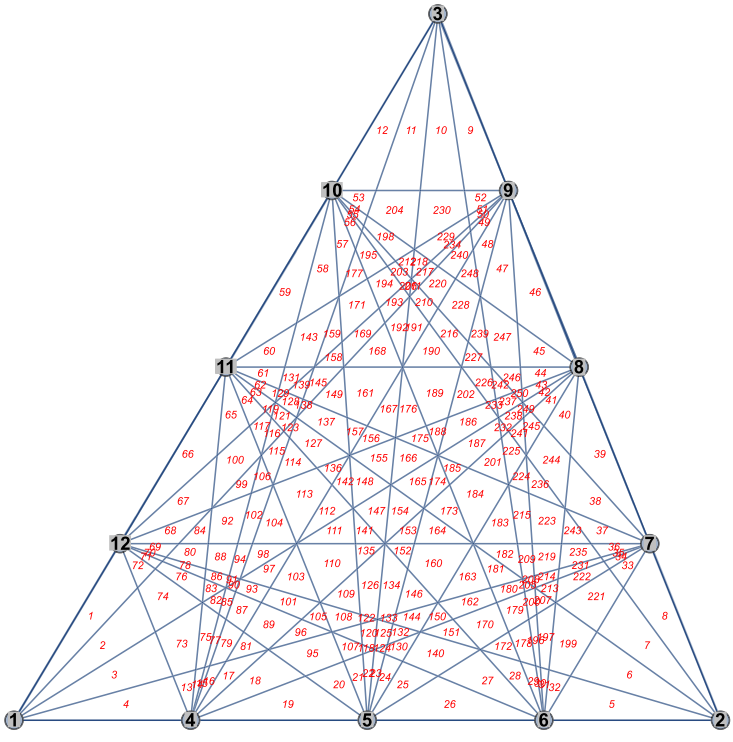

Fig. 3. A possible numbering of the 250 regions of the WS_4 split.

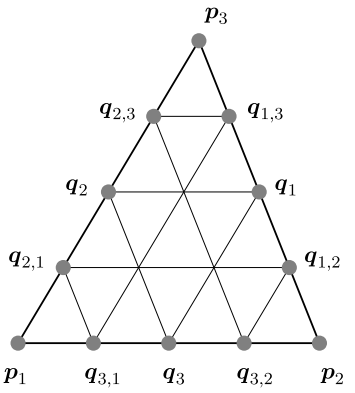

Fig. 4. Labeling of the knots on the boundary of the triangle Δ.

- *Recurrence relation (B-recurrence)*: For any $\boldsymbol{x} \in \mathbb{R}^e$ and any $b_1, \dots, b_{d+e+1}$ such that $\sum_i b_i \boldsymbol{\xi}_i = \boldsymbol{x}$, $\sum_i b_i = 1$, we have

$$M_\Xi(\boldsymbol{x}) = \frac{d+e}{d} \sum_{i=1}^{d+e+1} b_i M_{[\Xi \setminus \xi_i]}(\boldsymbol{x}).$$

- *Knot insertion formula (C-recurrence)*: For any $\boldsymbol{y} \in \mathbb{R}^e$ and any $c_1, \dots, c_{d+e+1}$ such that $\sum_i c_i \boldsymbol{\xi}_i = \boldsymbol{y}$, $\sum_i c_i = 1$, we have

$$M_\Xi = \sum_{i=1}^{d+e+1} c_i M_{[\Xi \cup \boldsymbol{y} \setminus \xi_i]}.$$

If $e = 1$ then M_Ξ is the univariate B-spline of degree d with knots Ξ, normalized to have its integral equal to one.

In the bivariate case, $e = 2$, the lines in the complete graph of Ξ are called *knot lines* and provide a partition of $\langle \Xi \rangle$ into polygonal elements. Denoting by $\#\Xi$ the cardinality of Ξ, the simplex spline M_Ξ is a polynomial of degree $d = \#\Xi - 3$ in each region of this partition. Across a knot line we have $M_\Xi \in C^{d+1-\mu}$, where μ is the number of knots on that knot line, including multiplicities.

3. A simplex spline basis for $\mathbb{S}_4^3(\Delta_{\mathrm{WS}_4})$

In this section, we focus on the space $\mathbb{S}_4^3(\Delta_{\mathrm{WS}_4})$; see (1) with $d = 4$. We provide a basis for the space consisting of scaled simplex splines and consider some properties of such a basis. With a slight abuse of notation we also refer to the basis functions as simplex splines. The simplex spline basis intrinsically takes care of the complex geometry of the WS_4 split by construction. Therefore, it provides a tool to practically deal with this quartic space.

3.1. A simplex spline basis

For a given triangle $\Delta = \langle \boldsymbol{p}_1, \boldsymbol{p}_2, \boldsymbol{p}_3 \rangle$, the WS_4 split is shown in the right plot of Fig. 1. From (2) we know that the dimension of $\mathbb{S}_4^3(\Delta_{\mathrm{WS}_4})$ is 51. In order to construct a basis for this space, we first specify 12 points along the boundary of the triangle (see Fig. 4): the three vertices $\boldsymbol{p}_1, \boldsymbol{p}_2, \boldsymbol{p}_3$, the points

$$\begin{aligned} \boldsymbol{q}_{1,2} &:= \frac{3}{4}\boldsymbol{p}_2 + \frac{1}{4}\boldsymbol{p}_3, \quad \boldsymbol{q}_{1,3} := \frac{1}{4}\boldsymbol{p}_2 + \frac{3}{4}\boldsymbol{p}_3, \\ \boldsymbol{q}_{2,1} &:= \frac{3}{4}\boldsymbol{p}_1 + \frac{1}{4}\boldsymbol{p}_3, \quad \boldsymbol{q}_{2,3} := \frac{1}{4}\boldsymbol{p}_1 + \frac{3}{4}\boldsymbol{p}_3, \\ \boldsymbol{q}_{3,1} &:= \frac{3}{4}\boldsymbol{p}_1 + \frac{1}{4}\boldsymbol{p}_2, \quad \boldsymbol{q}_{3,2} := \frac{1}{4}\boldsymbol{p}_1 + \frac{3}{4}\boldsymbol{p}_2, \end{aligned} \tag{3}$$

and the midpoints of the edges

$$\boldsymbol{q}_1 := \frac{1}{2}\boldsymbol{p}_2 + \frac{1}{2}\boldsymbol{p}_3, \quad \boldsymbol{q}_2 := \frac{1}{2}\boldsymbol{p}_1 + \frac{1}{2}\boldsymbol{p}_3, \quad \boldsymbol{q}_3 := \frac{1}{2}\boldsymbol{p}_1 + \frac{1}{2}\boldsymbol{p}_2. \tag{4}$$

Note that these points are part of the WS_4 split. We then consider the quartic simplex splines $M_1, \dots, M_{51}$ as schematically illustrated in Fig. 5, where each simplex spline has seven (including multiplicity) knots chosen among the 12 points above. For instance, M_4 is defined by the sequence

$$\{\boldsymbol{\xi}_1, \dots, \boldsymbol{\xi}_7\} = \{\boldsymbol{p}_1, \boldsymbol{p}_1, \boldsymbol{p}_1, \boldsymbol{p}_1, \boldsymbol{q}_{3,1}, \boldsymbol{q}_3, \boldsymbol{q}_{2,1}\}.$$

The B-recurrence relation may be used to compute each of them. We define the following set of 51 (scaled) simplex splines:

$$\mathcal{B} := \{B_i := w_i M_i,\ i = 1, \dots, 51\}, \tag{5}$$

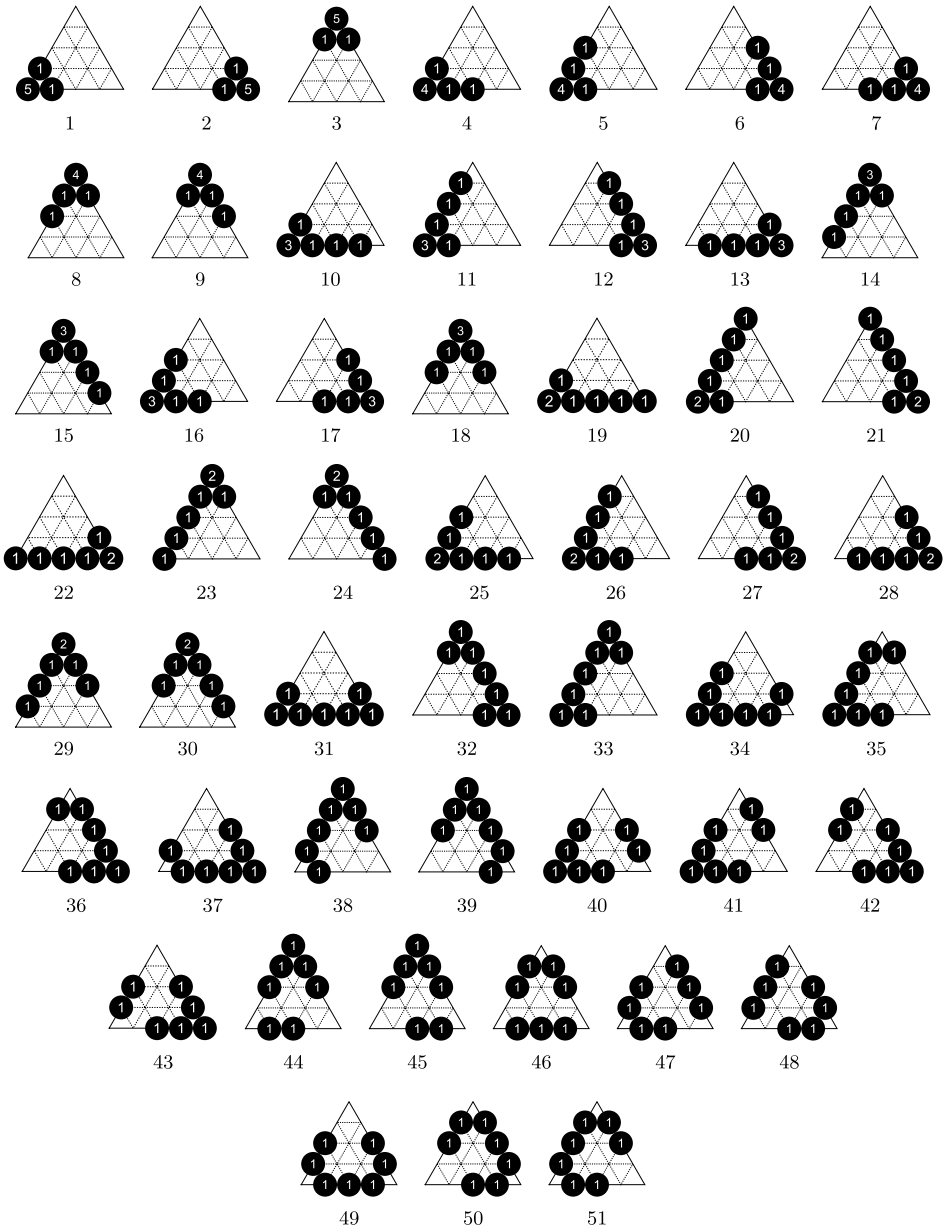

Fig. 5. Sequences of knots for a set of simplex spline basis functions for $\mathbb{S}_4^3(\Delta_{\mathrm{WS}_4})$. Each black disc shows the position of a knot and the number inside indicates its multiplicity.

with the scaling factors given by

$$w_i := \frac{|\Delta|}{480} \begin{cases} 2, & i = 1,2,3, \\ 4, & i = 4,\dots,9, \\ 6, & i = 10,\dots,15, \\ 8, & i = 16,\dots,24, \\ 12, & i = 25,\dots,30, \\ 14, & i = 31,32,33, \\ 18, & i = 34,\dots,39, \\ 8, & i = 40,\dots,45, \\ 9, & i = 46,47,48, \\ 15, & i = 49,50,51. \end{cases} \tag{6}$$

Here $|\Delta|$ stands for the area of Δ. Note that the scaling factors sum up to $|\Delta|$.

There are eleven different types of simplex splines in $\mathcal{B}$. For each type, a representative B_i is depicted in Figs. 11–21 in the appendix; the remaining ones can be obtained by symmetry. On any edge of Δ, there are eight nonzero basis functions. Their restrictions to that edge are nothing but the set of univariate C^3 quartic B-splines defined on a uniform open-knot sequence with three interior knots. For instance, for the edge $\boldsymbol{p}_1\boldsymbol{p}_2$, they correspond to the univariate quartic B-splines on the knot sequence specified by $\{\boldsymbol{p}_1,\boldsymbol{p}_1,\boldsymbol{p}_1,\boldsymbol{p}_1,\boldsymbol{p}_1,\boldsymbol{q}_{3,1},\boldsymbol{q}_3,\boldsymbol{q}_{3,2},\boldsymbol{p}_2,\boldsymbol{p}_2,\boldsymbol{p}_2,\boldsymbol{p}_2,\boldsymbol{p}_2\}$.

Theorem 1. *The simplex splines* $\{B_1,\dots,B_{51}\}$ *in* (5) *form a nonnegative partition of unity basis for the space* $\mathbb{S}_4^3(\Delta_{\mathrm{WS}_4})$.

Proof. Let B be one of the functions B_i. We first prove that B belongs to the space $\mathbb{S}_4^3(\Delta_{\mathrm{WS}_4})$. Since B has seven knots, it is a piecewise quartic polynomial. Moreover, since the knots of B are a subset of the knots shown in Fig. 4, the knot lines of B are a subset of the knot lines in the complete graph; see Fig. 1 (right). We also see that each interior knot line contains at most two knots, so B has C^3 smoothness according to the smoothness property of simplex splines; see Section 2.2. It follows that $B\in\mathbb{S}_4^3(\Delta_{\mathrm{WS}_4})$.

We now focus on the property of linear independence. Using the *ABC* formulas for simplex splines and the scaling factors in (6), we compute values and derivatives of B corresponding to the following 51 operators: $\rho_1,\dots,\rho_{30}$ are related to the vertices,

$$
\begin{aligned}
&\rho_1(f):=f(\boldsymbol{p}_1), && \rho_2(f):=f(\boldsymbol{p}_2), && \rho_3(f):=f(\boldsymbol{p}_3),\\
&\rho_4(f):=D_{\boldsymbol{p}_1\boldsymbol{p}_2}f(\boldsymbol{p}_1), && \rho_5(f):=D_{\boldsymbol{p}_1\boldsymbol{p}_3}f(\boldsymbol{p}_1), && \rho_6(f):=D_{\boldsymbol{p}_2\boldsymbol{p}_3}f(\boldsymbol{p}_2),\\
&\rho_7(f):=D_{\boldsymbol{p}_2\boldsymbol{p}_1}f(\boldsymbol{p}_2), && \rho_8(f):=D_{\boldsymbol{p}_3\boldsymbol{p}_1}f(\boldsymbol{p}_3), && \rho_9(f):=D_{\boldsymbol{p}_3\boldsymbol{p}_2}f(\boldsymbol{p}_3),\\
&\rho_{10}(f):=D^2_{\boldsymbol{p}_1\boldsymbol{p}_2}f(\boldsymbol{p}_1), && \rho_{11}(f):=D^2_{\boldsymbol{p}_1\boldsymbol{p}_3}f(\boldsymbol{p}_1), && \rho_{12}(f):=D^2_{\boldsymbol{p}_2\boldsymbol{p}_3}f(\boldsymbol{p}_2),\\
&\rho_{13}(f):=D^2_{\boldsymbol{p}_2\boldsymbol{p}_1}f(\boldsymbol{p}_2), && \rho_{14}(f):=D^2_{\boldsymbol{p}_3\boldsymbol{p}_1}f(\boldsymbol{p}_3), && \rho_{15}(f):=D^2_{\boldsymbol{p}_3\boldsymbol{p}_2}f(\boldsymbol{p}_3),\\
&\rho_{16}(f):=D_{\boldsymbol{p}_1\boldsymbol{p}_2}D_{\boldsymbol{p}_1\boldsymbol{p}_3}f(\boldsymbol{p}_1), && \rho_{17}(f):=D_{\boldsymbol{p}_2\boldsymbol{p}_3}D_{\boldsymbol{p}_2\boldsymbol{p}_1}f(\boldsymbol{p}_2), && \rho_{18}(f):=D_{\boldsymbol{p}_3\boldsymbol{p}_1}D_{\boldsymbol{p}_3\boldsymbol{p}_2}f(\boldsymbol{p}_3),\\
&\rho_{19}(f):=D^3_{\boldsymbol{p}_1\boldsymbol{p}_2}f(\boldsymbol{p}_1), && \rho_{20}(f):=D^3_{\boldsymbol{p}_1\boldsymbol{p}_3}f(\boldsymbol{p}_1), && \rho_{21}(f):=D^3_{\boldsymbol{p}_2\boldsymbol{p}_3}f(\boldsymbol{p}_2),\\
&\rho_{22}(f):=D^3_{\boldsymbol{p}_2\boldsymbol{p}_1}f(\boldsymbol{p}_2), && \rho_{23}(f):=D^3_{\boldsymbol{p}_3\boldsymbol{p}_1}f(\boldsymbol{p}_3), && \rho_{24}(f):=D^3_{\boldsymbol{p}_3\boldsymbol{p}_2}f(\boldsymbol{p}_3),\\
&\rho_{25}(f):=D^2_{\boldsymbol{p}_1\boldsymbol{p}_2}D_{\boldsymbol{p}_1\boldsymbol{p}_3}f(\boldsymbol{p}_1), && \rho_{26}(f):=D^2_{\boldsymbol{p}_1\boldsymbol{p}_3}D_{\boldsymbol{p}_1\boldsymbol{p}_2}f(\boldsymbol{p}_1), && \rho_{27}(f):=D^2_{\boldsymbol{p}_2\boldsymbol{p}_3}D_{\boldsymbol{p}_2\boldsymbol{p}_1}f(\boldsymbol{p}_2),\\
&\rho_{28}(f):=D^2_{\boldsymbol{p}_2\boldsymbol{p}_1}D_{\boldsymbol{p}_2\boldsymbol{p}_3}f(\boldsymbol{p}_2), && \rho_{29}(f):=D^2_{\boldsymbol{p}_3\boldsymbol{p}_1}D_{\boldsymbol{p}_3\boldsymbol{p}_2}f(\boldsymbol{p}_3), && \rho_{30}(f):=D^2_{\boldsymbol{p}_3\boldsymbol{p}_2}D_{\boldsymbol{p}_3\boldsymbol{p}_1}f(\boldsymbol{p}_3);
\end{aligned}
\tag{7}
$$

$\rho_{31},\dots,\rho_{48}$ are related to the edges,

$$
\begin{aligned}
&\rho_{31}(f):=D_{\boldsymbol{q}_3\boldsymbol{p}_3}f(\boldsymbol{q}_3), && \rho_{32}(f):=D_{\boldsymbol{q}_1\boldsymbol{p}_1}f(\boldsymbol{q}_1), && \rho_{33}(f):=D_{\boldsymbol{q}_2\boldsymbol{p}_2}f(\boldsymbol{q}_2),\\
&\rho_{34}(f):=D^2_{\boldsymbol{q}_{3,1}\boldsymbol{p}_3}f(\boldsymbol{q}_{3,1}), && \rho_{35}(f):=D^2_{\boldsymbol{q}_{2,1}\boldsymbol{p}_2}f(\boldsymbol{q}_{2,1}), && \rho_{36}(f):=D^2_{\boldsymbol{q}_{1,2}\boldsymbol{p}_1}f(\boldsymbol{q}_{1,2}),\\
&\rho_{37}(f):=D^2_{\boldsymbol{q}_{3,2}\boldsymbol{p}_3}f(\boldsymbol{q}_{3,2}), && \rho_{38}(f):=D^2_{\boldsymbol{q}_{2,3}\boldsymbol{p}_2}f(\boldsymbol{q}_{2,3}), && \rho_{39}(f):=D^2_{\boldsymbol{q}_{1,3}\boldsymbol{p}_1}f(\boldsymbol{q}_{1,3}),\\
&\rho_{40}(f):=D^3_{\boldsymbol{q}_{3,1}\boldsymbol{p}_3}f(\boldsymbol{q}_{3,1}), && \rho_{41}(f):=D^3_{\boldsymbol{q}_{2,1}\boldsymbol{p}_2}f(\boldsymbol{q}_{2,1}), && \rho_{42}(f):=D^3_{\boldsymbol{q}_{1,2}\boldsymbol{p}_1}f(\boldsymbol{q}_{1,2}),\\
&\rho_{43}(f):=D^3_{\boldsymbol{q}_{3,2}\boldsymbol{p}_3}f(\boldsymbol{q}_{3,2}), && \rho_{44}(f):=D^3_{\boldsymbol{q}_{2,3}\boldsymbol{p}_2}f(\boldsymbol{q}_{2,3}), && \rho_{45}(f):=D^3_{\boldsymbol{q}_{1,3}\boldsymbol{p}_1}f(\boldsymbol{q}_{1,3}),\\
&\rho_{46}(f):=D^3_{\boldsymbol{q}_3\boldsymbol{p}_3}f(\boldsymbol{q}_3), && \rho_{47}(f):=D^3_{\boldsymbol{q}_1\boldsymbol{p}_1}f(\boldsymbol{q}_1), && \rho_{48}(f):=D^3_{\boldsymbol{q}_2\boldsymbol{p}_2}f(\boldsymbol{q}_2);
\end{aligned}
\tag{8}
$$

and the final ρ_{49}, ρ_{50}, and ρ_{51} are related to the triangle,

$$
\rho_{49}(f):=f(\boldsymbol{v}_3),\quad \rho_{50}(f):=f(\boldsymbol{v}_1),\quad \rho_{51}(f):=f(\boldsymbol{v}_2),
\tag{9}
$$

where

$$
\boldsymbol{v}_3:=\frac{3}{8}\boldsymbol{p}_1+\frac{3}{8}\boldsymbol{p}_2+\frac{1}{4}\boldsymbol{p}_3,\quad \boldsymbol{v}_1:=\frac{3}{8}\boldsymbol{p}_2+\frac{3}{8}\boldsymbol{p}_3+\frac{1}{4}\boldsymbol{p}_1,\quad \boldsymbol{v}_2:=\frac{3}{8}\boldsymbol{p}_3+\frac{3}{8}\boldsymbol{p}_1+\frac{1}{4}\boldsymbol{p}_2.
\tag{10}
$$

The computed values are shown in Tables 3–5 in the appendix. The matrix $[\rho_j(B_i)]\in\mathbb{R}^{51\times51}$ is block triangular with nonsingular diagonal blocks, so linear independence of the set of functions $\{B_1,\dots,B_{51}\}$ follows. As a consequence, due to (2), these functions form a basis of the space $\mathbb{S}_4^3(\Delta_{\mathrm{WS}_4})$. At the same time, we may conclude linear independence of the set of operators $\{\rho_1,\dots,\rho_{51}\}$ defined on $\mathbb{S}_4^3(\Delta_{\mathrm{WS}_4})$.

Simplex splines are nonnegative, so it only remains to prove that the functions in (5) sum up to one on Δ. A direct inspection of Tables 3–5 shows that

$$
\rho_j\left(\sum_{i=1}^{51}B_i\right)=\sum_{i=1}^{51}\rho_j(B_i)=\rho_j(1),\quad j=1,\dots,51.
$$

Since the operators ρ_j are linearly independent, $\sum_{i=1}^{51}B_i$ must be equal to the unity function which belongs to $\mathbb{S}_4^3(\Delta_{\mathrm{WS}_4})$. □

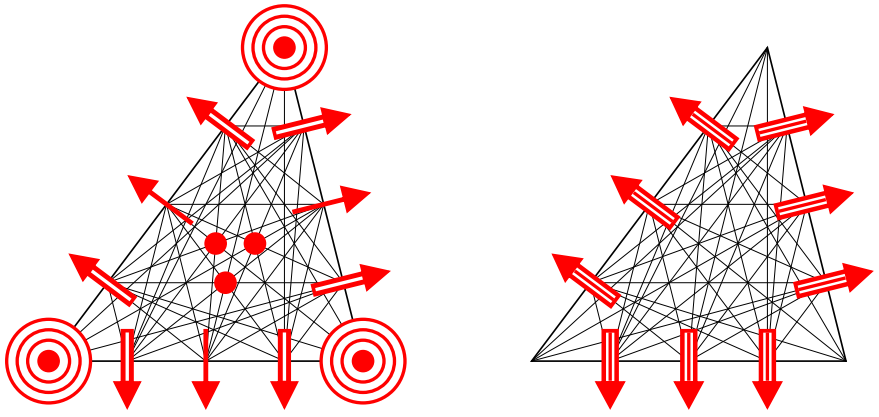

Fig. 6. Hermite degrees of freedom on the WS_4 split. Left: (11), (12), (13), and (16). Right: (14) and (15).

The proof of Theorem 1 implies that we can formulate a Hermite interpolation problem to characterize any spline in $\mathbb{S}_4^3(\Delta_{\mathrm{WS}_4})$; see also [31, Theorem 7.28].

Corollary 2. *For given data $f_{k,\alpha,\beta}$, g_k, $g_{k,l}$, $\bar{g}_k$, $\bar{g}_{k,l}$, and h_k there exists a unique spline $s \in \mathbb{S}_4^3(\Delta_{\mathrm{WS}_4})$ such that*

$$D_x^\alpha D_y^\beta s(\boldsymbol{p}_k) = f_{k,\alpha,\beta}, \quad 0 \le \alpha+\beta \le 3, \quad k=1,2,3, \tag{11}$$

$$D_{\boldsymbol{n}_k} s(\boldsymbol{q}_k) = g_k, \qquad k=1,2,3, \tag{12}$$

$$D_{\boldsymbol{n}_k}^2 s(\boldsymbol{q}_{k,l}) = g_{k,l}, \qquad k,l=1,2,3, \quad k\neq l, \tag{13}$$

$$D_{\boldsymbol{n}_k}^3 s(\boldsymbol{q}_k) = \bar{g}_k, \qquad k=1,2,3, \tag{14}$$

$$D_{\boldsymbol{n}_k}^3 s(\boldsymbol{q}_{k,l}) = \bar{g}_{k,l}, \qquad k,l=1,2,3, \quad k\neq l, \tag{15}$$

$$s(\boldsymbol{v}_k) = h_k, \qquad k=1,2,3, \tag{16}$$

where $\boldsymbol{n}_k$ is the normal (or any nonparallel) direction of the edge opposite to vertex $\boldsymbol{p}_k$, and the points $\boldsymbol{q}_{k,l}$, $\boldsymbol{q}_k$, and $\boldsymbol{v}_k$ are defined in (3), (4), and (10), respectively.

A schematic visualization of the Hermite degrees of freedom specified in Corollary 2 is shown in Fig. 6 using graphical symbols that are common in finite element literature; see, e.g., [3].

3.2. Domain points

For the scaled simplex spline basis (5), we now compute special points in Δ that are often used in geometric modeling to give a geometric interpretation to the representation of any element of $\mathbb{S}_4^3(\Delta_{\mathrm{WS}_4})$ in terms of the considered spline basis. To this end, we solve the system

$$\rho_j\left(\sum_{i=1}^{51} b_i^*(f)B_i\right) = \rho_j(f)$$

for the two functions $f_1(x,y) := x$ and $f_2(x,y) := y$. The points

$$\boldsymbol{b}_i^* := (b_i^*(f_1), b_i^*(f_2)), \quad i=1,\dots,51, \tag{17}$$

are called the *domain points* of the basis (5). Together with the partition of unity, the domain points provide an explicit representation of any affine function with respect to the basis (5). The barycentric coordinates with respect to the triangle Δ of the domain points (17), multiplied by the common factor 336, are given by

$$\begin{aligned}
&\boldsymbol{b}_1^* : (336,0,0), && \boldsymbol{b}_2^* : (0,336,0), && \boldsymbol{b}_3^* : (0,0,336),\\
&\boldsymbol{b}_4^* : (315,21,0), && \boldsymbol{b}_5^* : (315,0,21), && \boldsymbol{b}_6^* : (0,315,21),\\
&\boldsymbol{b}_7^* : (21,315,0), && \boldsymbol{b}_8^* : (21,0,315), && \boldsymbol{b}_9^* : (0,21,315),\\
&\boldsymbol{b}_{10}^* : (273,63,0), && \boldsymbol{b}_{11}^* : (273,0,63), && \boldsymbol{b}_{12}^* : (0,273,63),\\
&\boldsymbol{b}_{13}^* : (63,273,0), && \boldsymbol{b}_{14}^* : (63,0,273), && \boldsymbol{b}_{15}^* : (0,63,273),
\end{aligned}$$

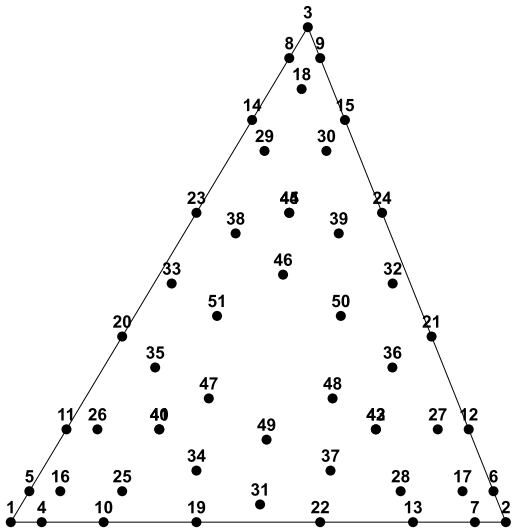

Fig. 7. The domain points given by (18) for $\mathbb{S}_4^3(\Delta_{\mathrm{WS}_4})$. Only 48 distinct points are depicted; there are three pairs of coincident points, namely $\{\boldsymbol{b}^*_{40}, \boldsymbol{b}^*_{41}\}$, $\{\boldsymbol{b}^*_{42}, \boldsymbol{b}^*_{43}\}$, and $\{\boldsymbol{b}^*_{44}, \boldsymbol{b}^*_{45}\}$.

$$
\begin{aligned}
&\boldsymbol{b}^*_{16} : (294,21,21), && \boldsymbol{b}^*_{17} : (21,294,21), && \boldsymbol{b}^*_{18} : (21,21,294),\\
&\boldsymbol{b}^*_{19} : (210,126,0), && \boldsymbol{b}^*_{20} : (210,0,126), && \boldsymbol{b}^*_{21} : (0,210,126),\\
&\boldsymbol{b}^*_{22} : (126,210,0), && \boldsymbol{b}^*_{23} : (126,0,210), && \boldsymbol{b}^*_{24} : (0,126,210),\\
&\boldsymbol{b}^*_{25} : (252,63,21), && \boldsymbol{b}^*_{26} : (252,21,63), && \boldsymbol{b}^*_{27} : (21,252,63),\\
&\boldsymbol{b}^*_{28} : (63,252,21), && \boldsymbol{b}^*_{29} : (63,21,252), && \boldsymbol{b}^*_{30} : (21,63,252),\\
&\boldsymbol{b}^*_{31} : (162,162,12), && \boldsymbol{b}^*_{32} : (12,162,162), && \boldsymbol{b}^*_{33} : (162,12,162),\\
&\boldsymbol{b}^*_{34} : (196,105,35), && \boldsymbol{b}^*_{35} : (196,35,105), && \boldsymbol{b}^*_{36} : (35,195,105),\\
&\boldsymbol{b}^*_{37} : (105,196,35), && \boldsymbol{b}^*_{38} : (105,35,196), && \boldsymbol{b}^*_{39} : (35,105,196),\\
&\boldsymbol{b}^*_{40} : (210,63,63), && \boldsymbol{b}^*_{41} : (210,63,63), && \boldsymbol{b}^*_{42} : (63,210,63),\\
&\boldsymbol{b}^*_{43} : (63,210,63), && \boldsymbol{b}^*_{44} : (63,63,210), && \boldsymbol{b}^*_{45} : (63,63,210),\\
&\boldsymbol{b}^*_{46} : (84,84,168), && \boldsymbol{b}^*_{47} : (168,84,84), && \boldsymbol{b}^*_{48} : (84,168,84),\\
&\boldsymbol{b}^*_{49} : (140,140,56), && \boldsymbol{b}^*_{50} : (56,140,140), && \boldsymbol{b}^*_{51} : (140,56,140).
\end{aligned}
\tag{18}
$$

These points are depicted in Fig. 7. When representing a spline $s \in \mathbb{S}_4^3(\Delta_{\mathrm{WS}_4})$ in the basis (5),

$$
s = \sum_{i=1}^{51} b_i B_i, \tag{19}
$$

the corresponding *control points* are defined as $(\boldsymbol{b}^*_i, b_i)$, $i = 1, \dots, 51$ which are usually connected into a *control net*. Unfortunately, the domain points in (18) are not all distinct; there are three pairs of coincident points, namely $\{\boldsymbol{b}^*_{40}, \boldsymbol{b}^*_{41}\}$, $\{\boldsymbol{b}^*_{42}, \boldsymbol{b}^*_{43}\}$, and $\{\boldsymbol{b}^*_{44}, \boldsymbol{b}^*_{45}\}$. This makes their use of limited interest in geometric modeling.

3.3. A Marsden-like identity

We now provide a Marsden-like identity to represent any quartic polynomial with respect to the scaled simplex spline basis (5). The results are obtained by direct computation.

Theorem 3. *Given the triangle $\Delta = \langle \boldsymbol{p}_1, \boldsymbol{p}_2, \boldsymbol{p}_3 \rangle$, we first introduce the points*

$$
\begin{aligned}
&\boldsymbol{u}_1 := \tfrac{1}{7}\boldsymbol{p}_1 + \tfrac{3}{7}\boldsymbol{p}_2 + \tfrac{3}{7}\boldsymbol{p}_3, \quad \boldsymbol{u}_2 := \tfrac{3}{7}\boldsymbol{p}_1 + \tfrac{1}{7}\boldsymbol{p}_2 + \tfrac{3}{7}\boldsymbol{p}_3, \quad \boldsymbol{u}_3 := \tfrac{3}{7}\boldsymbol{p}_1 + \tfrac{3}{7}\boldsymbol{p}_2 + \tfrac{1}{7}\boldsymbol{p}_3,\\
&\boldsymbol{w}_1 := \tfrac{1}{3}\boldsymbol{p}_1 + \tfrac{1}{2}\boldsymbol{p}_2 + \tfrac{1}{6}\boldsymbol{p}_3, \quad \boldsymbol{w}_2 := \tfrac{1}{3}\boldsymbol{p}_1 + \tfrac{1}{6}\boldsymbol{p}_2 + \tfrac{1}{2}\boldsymbol{p}_3, \quad \boldsymbol{w}_3 := \tfrac{1}{6}\boldsymbol{p}_1 + \tfrac{1}{3}\boldsymbol{p}_2 + \tfrac{1}{2}\boldsymbol{p}_3,\\
&\boldsymbol{w}_4 := \tfrac{1}{2}\boldsymbol{p}_1 + \tfrac{1}{3}\boldsymbol{p}_2 + \tfrac{1}{6}\boldsymbol{p}_3, \quad \boldsymbol{w}_5 := \tfrac{1}{2}\boldsymbol{p}_1 + \tfrac{1}{6}\boldsymbol{p}_2 + \tfrac{1}{3}\boldsymbol{p}_3, \quad \boldsymbol{w}_6 := \tfrac{1}{6}\boldsymbol{p}_1 + \tfrac{1}{2}\boldsymbol{p}_2 + \tfrac{1}{3}\boldsymbol{p}_3,
\end{aligned}
$$

Table 1
The dual points $\boldsymbol{r}_{i,j}$, $i = 1,\dots,48$, $j = 1,\dots,4$ used in the Marsden-like identity (20).

i	1	2	3	4	5	6	7	8	9	10	11	12
$\boldsymbol{r}_{i,1}$	$\boldsymbol{p}_1$	$\boldsymbol{p}_2$	$\boldsymbol{p}_3$	$\boldsymbol{p}_1$	$\boldsymbol{p}_1$	$\boldsymbol{p}_2$	$\boldsymbol{p}_2$	$\boldsymbol{p}_3$	$\boldsymbol{p}_3$	$\boldsymbol{p}_1$	$\boldsymbol{p}_1$	$\boldsymbol{p}_2$
$\boldsymbol{r}_{i,2}$	$\boldsymbol{p}_1$	$\boldsymbol{p}_2$	$\boldsymbol{p}_3$	$\boldsymbol{p}_1$	$\boldsymbol{p}_1$	$\boldsymbol{p}_2$	$\boldsymbol{p}_2$	$\boldsymbol{p}_3$	$\boldsymbol{p}_3$	$\boldsymbol{p}_1$	$\boldsymbol{p}_1$	$\boldsymbol{p}_2$
$\boldsymbol{r}_{i,3}$	$\boldsymbol{p}_1$	$\boldsymbol{p}_2$	$\boldsymbol{p}_3$	$\boldsymbol{p}_1$	$\boldsymbol{p}_1$	$\boldsymbol{p}_2$	$\boldsymbol{p}_2$	$\boldsymbol{p}_3$	$\boldsymbol{p}_3$	$\boldsymbol{q}_{3,1}$	$\boldsymbol{q}_{2,1}$	$\boldsymbol{q}_{1,2}$
$\boldsymbol{r}_{i,4}$	$\boldsymbol{p}_1$	$\boldsymbol{p}_2$	$\boldsymbol{p}_3$	$\boldsymbol{q}_{3,1}$	$\boldsymbol{q}_{2,1}$	$\boldsymbol{q}_{1,2}$	$\boldsymbol{q}_{3,2}$	$\boldsymbol{q}_{2,3}$	$\boldsymbol{q}_{1,3}$	$\boldsymbol{q}_3$	$\boldsymbol{q}_2$	$\boldsymbol{q}_1$

i	13	14	15	16	17	18	19	20	21	22	23	24
$\boldsymbol{r}_{i,1}$	$\boldsymbol{p}_2$	$\boldsymbol{p}_3$	$\boldsymbol{p}_3$	$\boldsymbol{p}_1$	$\boldsymbol{p}_2$	$\boldsymbol{p}_3$	$\boldsymbol{p}_1$	$\boldsymbol{p}_1$	$\boldsymbol{p}_2$	$\boldsymbol{p}_2$	$\boldsymbol{p}_3$	$\boldsymbol{p}_3$
$\boldsymbol{r}_{i,2}$	$\boldsymbol{p}_2$	$\boldsymbol{p}_3$	$\boldsymbol{p}_3$	$\boldsymbol{p}_1$	$\boldsymbol{p}_2$	$\boldsymbol{p}_3$	$\boldsymbol{q}_3$	$\boldsymbol{q}_2$	$\boldsymbol{q}_1$	$\boldsymbol{q}_3$	$\boldsymbol{q}_2$	$\boldsymbol{q}_1$
$\boldsymbol{r}_{i,3}$	$\boldsymbol{q}_{3,2}$	$\boldsymbol{q}_{2,3}$	$\boldsymbol{q}_{1,3}$	$\boldsymbol{q}_{3,1}$	$\boldsymbol{q}_{3,2}$	$\boldsymbol{q}_{1,3}$	$\boldsymbol{q}_{3,1}$	$\boldsymbol{q}_{2,3}$	$\boldsymbol{q}_{1,2}$	$\boldsymbol{q}_{3,1}$	$\boldsymbol{q}_{2,3}$	$\boldsymbol{q}_{1,2}$
$\boldsymbol{r}_{i,4}$	$\boldsymbol{q}_3$	$\boldsymbol{q}_2$	$\boldsymbol{q}_1$	$\boldsymbol{q}_{2,1}$	$\boldsymbol{q}_{1,2}$	$\boldsymbol{q}_{2,3}$	$\boldsymbol{q}_{3,2}$	$\boldsymbol{q}_{2,1}$	$\boldsymbol{q}_{1,3}$	$\boldsymbol{q}_{3,2}$	$\boldsymbol{q}_{2,1}$	$\boldsymbol{q}_{1,3}$

i	25	26	27	28	29	30	31	32	33	34	35	36
$\boldsymbol{r}_{i,1}$	$\boldsymbol{p}_1$	$\boldsymbol{p}_1$	$\boldsymbol{p}_2$	$\boldsymbol{p}_2$	$\boldsymbol{p}_3$	$\boldsymbol{p}_3$	$\boldsymbol{q}_3$	$\boldsymbol{q}_1$	$\boldsymbol{q}_2$	$\boldsymbol{q}_3$	$\boldsymbol{q}_2$	$\boldsymbol{q}_1$
$\boldsymbol{r}_{i,2}$	$\boldsymbol{q}_3$	$\boldsymbol{q}_2$	$\boldsymbol{q}_1$	$\boldsymbol{q}_3$	$\boldsymbol{q}_2$	$\boldsymbol{q}_1$	$\boldsymbol{q}_{3,1}$	$\boldsymbol{q}_{1,2}$	$\boldsymbol{q}_{2,3}$	$\boldsymbol{q}_{3,1}$	$\boldsymbol{q}_{3,1}$	$\boldsymbol{q}_{3,2}$
$\boldsymbol{r}_{i,3}$	$\boldsymbol{q}_{3,1}$	$\boldsymbol{q}_{3,1}$	$\boldsymbol{q}_{3,2}$	$\boldsymbol{q}_{3,2}$	$\boldsymbol{q}_{1,3}$	$\boldsymbol{q}_{1,3}$	$\boldsymbol{q}_{3,2}$	$\boldsymbol{q}_{1,3}$	$\boldsymbol{q}_{2,1}$	$\boldsymbol{q}_{2,1}$	$\boldsymbol{q}_{2,1}$	$\boldsymbol{q}_{1,2}$
$\boldsymbol{r}_{i,4}$	$\boldsymbol{q}_{2,1}$	$\boldsymbol{q}_{2,1}$	$\boldsymbol{q}_{1,2}$	$\boldsymbol{q}_{1,2}$	$\boldsymbol{q}_{2,3}$	$\boldsymbol{q}_{2,3}$	$\boldsymbol{u}_3$	$\boldsymbol{u}_1$	$\boldsymbol{u}_2$	$\boldsymbol{w}_1$	$\boldsymbol{w}_2$	$\boldsymbol{w}_3$

i	37	38	39	40	41	42	43	44	45	46	47	48
$\boldsymbol{r}_{i,1}$	$\boldsymbol{q}_3$	$\boldsymbol{q}_2$	$\boldsymbol{q}_1$	$\boldsymbol{q}_2$	$\boldsymbol{q}_2$	$\boldsymbol{q}_1$	$\boldsymbol{q}_1$	$\boldsymbol{q}_1$	$\boldsymbol{q}_1$	$\boldsymbol{p}_3$	$\boldsymbol{p}_1$	$\boldsymbol{p}_2$
$\boldsymbol{r}_{i,2}$	$\boldsymbol{q}_{3,2}$	$\boldsymbol{q}_{1,3}$	$\boldsymbol{q}_{1,3}$	$\boldsymbol{q}_{3,1}$	$\boldsymbol{q}_{3,1}$	$\boldsymbol{q}_{3,2}$	$\boldsymbol{q}_{3,2}$	$\boldsymbol{q}_{1,3}$	$\boldsymbol{q}_{1,3}$	$\boldsymbol{q}_1$	$\boldsymbol{q}_1$	$\boldsymbol{q}_1$
$\boldsymbol{r}_{i,3}$	$\boldsymbol{q}_{1,2}$	$\boldsymbol{q}_{2,3}$	$\boldsymbol{q}_{2,3}$	$\boldsymbol{q}_{2,1}$	$\boldsymbol{q}_{2,1}$	$\boldsymbol{q}_{1,2}$	$\boldsymbol{q}_{1,2}$	$\boldsymbol{q}_{2,3}$	$\boldsymbol{q}_{2,3}$	$\boldsymbol{q}_2$	$\boldsymbol{q}_2$	$\boldsymbol{q}_2$
$\boldsymbol{r}_{i,4}$	$\boldsymbol{w}_4$	$\boldsymbol{w}_5$	$\boldsymbol{w}_6$	$\boldsymbol{q}_3$	$\boldsymbol{q}_3$	$\boldsymbol{q}_3$	$\boldsymbol{q}_3$	$\boldsymbol{q}_2$	$\boldsymbol{q}_2$	$\boldsymbol{q}_3$	$\boldsymbol{q}_3$	$\boldsymbol{q}_3$

and recall the points $\boldsymbol{q}_{i,j}$ and $\boldsymbol{q}_i$ defined in (3) and (4), respectively. We have the identity

$$(1+\boldsymbol{y}^T\boldsymbol{x})^4 = \sum_{i=1}^{51} \psi_i(\boldsymbol{y}) B_i(\boldsymbol{x}), \quad \boldsymbol{y}\in\mathbb{R}^2, \quad \boldsymbol{x}\in\Delta, \tag{20}$$

where the functions ψ_i are called dual polynomials. The first 48 dual polynomials can be written in the form

$$\psi_i(\boldsymbol{y}) := (1+\boldsymbol{y}^T\boldsymbol{r}_{i,1})(1+\boldsymbol{y}^T\boldsymbol{r}_{i,2})(1+\boldsymbol{y}^T\boldsymbol{r}_{i,3})(1+\boldsymbol{y}^T\boldsymbol{r}_{i,4}), \quad i=1,\dots,48$$

in terms of the dual points $\boldsymbol{r}_{i,j}$ specified in Table 1, and

$$\begin{aligned}
\psi_{49}(\boldsymbol{y}) :=\ & (1+\boldsymbol{y}^T\boldsymbol{q}_3)\Big(-\frac{32}{5}(1+\boldsymbol{y}^T\boldsymbol{q}_3)^3+\frac{11}{15}(1+\boldsymbol{y}^T\boldsymbol{q}_{3,1})(1+\boldsymbol{y}^T\boldsymbol{q}_3)(1+\boldsymbol{y}^T\boldsymbol{q}_{3,2})\\
&+\frac{29}{5}(1+\boldsymbol{y}^T\boldsymbol{q}_3)(1+\boldsymbol{y}^T\boldsymbol{q}_{3,2})(1+\boldsymbol{y}^T\boldsymbol{q}_{1,2})-\frac{59}{15}(1+\boldsymbol{y}^T\boldsymbol{q}_{3,2})(1+\boldsymbol{y}^T\boldsymbol{q}_{1,2})(1+\boldsymbol{y}^T\boldsymbol{q}_1)\\
&+\frac{11}{5}(1+\boldsymbol{y}^T\boldsymbol{q}_{1,2})(1+\boldsymbol{y}^T\boldsymbol{q}_1)(1+\boldsymbol{y}^T\boldsymbol{q}_{1,3})-\frac{11}{15}(1+\boldsymbol{y}^T\boldsymbol{q}_1)(1+\boldsymbol{y}^T\boldsymbol{q}_{1,3})(1+\boldsymbol{y}^T\boldsymbol{q}_{2,3})\\
&-\frac{11}{15}(1+\boldsymbol{y}^T\boldsymbol{q}_{1,3})(1+\boldsymbol{y}^T\boldsymbol{q}_{2,3})(1+\boldsymbol{y}^T\boldsymbol{q}_2)+\frac{29}{5}(1+\boldsymbol{y}^T\boldsymbol{q}_{3,1})(1+\boldsymbol{y}^T\boldsymbol{q}_3)(1+\boldsymbol{y}^T\boldsymbol{q}_{2,1})\\
&-\frac{59}{15}(1+\boldsymbol{y}^T\boldsymbol{q}_{3,1})(1+\boldsymbol{y}^T\boldsymbol{q}_2)(1+\boldsymbol{y}^T\boldsymbol{q}_{2,1})+\frac{11}{5}(1+\boldsymbol{y}^T\boldsymbol{q}_{2,3})(1+\boldsymbol{y}^T\boldsymbol{q}_2)(1+\boldsymbol{y}^T\boldsymbol{q}_{2,1})\Big),\\
\psi_{50}(\boldsymbol{y}) :=\ & (1+\boldsymbol{y}^T\boldsymbol{q}_1)\Big(-\frac{32}{5}(1+\boldsymbol{y}^T\boldsymbol{q}_1)^3+\frac{11}{5}(1+\boldsymbol{y}^T\boldsymbol{q}_{3,1})(1+\boldsymbol{y}^T\boldsymbol{q}_3)(1+\boldsymbol{y}^T\boldsymbol{q}_{3,2})\\
&-\frac{59}{15}(1+\boldsymbol{y}^T\boldsymbol{q}_3)(1+\boldsymbol{y}^T\boldsymbol{q}_{3,2})(1+\boldsymbol{y}^T\boldsymbol{q}_{1,2})+\frac{29}{5}(1+\boldsymbol{y}^T\boldsymbol{q}_{3,2})(1+\boldsymbol{y}^T\boldsymbol{q}_{1,2})(1+\boldsymbol{y}^T\boldsymbol{q}_1)\\
&+\frac{11}{15}(1+\boldsymbol{y}^T\boldsymbol{q}_{1,2})(1+\boldsymbol{y}^T\boldsymbol{q}_1)(1+\boldsymbol{y}^T\boldsymbol{q}_{1,3})+\frac{29}{5}(1+\boldsymbol{y}^T\boldsymbol{q}_1)(1+\boldsymbol{y}^T\boldsymbol{q}_{1,3})(1+\boldsymbol{y}^T\boldsymbol{q}_{2,3})\\
&-\frac{59}{15}(1+\boldsymbol{y}^T\boldsymbol{q}_{1,3})(1+\boldsymbol{y}^T\boldsymbol{q}_{2,3})(1+\boldsymbol{y}^T\boldsymbol{q}_2)-\frac{11}{15}(1+\boldsymbol{y}^T\boldsymbol{q}_{3,1})(1+\boldsymbol{y}^T\boldsymbol{q}_3)(1+\boldsymbol{y}^T\boldsymbol{q}_{2,1})\\
&-\frac{11}{15}(1+\boldsymbol{y}^T\boldsymbol{q}_{3,1})(1+\boldsymbol{y}^T\boldsymbol{q}_2)(1+\boldsymbol{y}^T\boldsymbol{q}_{2,1})+\frac{11}{5}(1+\boldsymbol{y}^T\boldsymbol{q}_{2,3})(1+\boldsymbol{y}^T\boldsymbol{q}_2)(1+\boldsymbol{y}^T\boldsymbol{q}_{2,1})\Big),\\
\psi_{51}(\boldsymbol{y}) :=\ & (1+\boldsymbol{y}^T\boldsymbol{q}_2)\Big(-\frac{32}{5}(1+\boldsymbol{y}^T\boldsymbol{q}_2)^3+\frac{11}{5}(1+\boldsymbol{y}^T\boldsymbol{q}_{3,1})(1+\boldsymbol{y}^T\boldsymbol{q}_3)(1+\boldsymbol{y}^T\boldsymbol{q}_{3,2})\\
&-\frac{11}{15}(1+\boldsymbol{y}^T\boldsymbol{q}_3)(1+\boldsymbol{y}^T\boldsymbol{q}_{3,2})(1+\boldsymbol{y}^T\boldsymbol{q}_{1,2})-\frac{11}{15}(1+\boldsymbol{y}^T\boldsymbol{q}_{3,2})(1+\boldsymbol{y}^T\boldsymbol{q}_{1,2})(1+\boldsymbol{y}^T\boldsymbol{q}_1)\\
&+\frac{11}{5}(1+\boldsymbol{y}^T\boldsymbol{q}_{1,2})(1+\boldsymbol{y}^T\boldsymbol{q}_1)(1+\boldsymbol{y}^T\boldsymbol{q}_{1,3})-\frac{59}{15}(1+\boldsymbol{y}^T\boldsymbol{q}_1)(1+\boldsymbol{y}^T\boldsymbol{q}_{1,3})(1+\boldsymbol{y}^T\boldsymbol{q}_{2,3})\\
&+\frac{29}{5}(1+\boldsymbol{y}^T\boldsymbol{q}_{1,3})(1+\boldsymbol{y}^T\boldsymbol{q}_{2,3})(1+\boldsymbol{y}^T\boldsymbol{q}_2)-\frac{59}{15}(1+\boldsymbol{y}^T\boldsymbol{q}_{3,1})(1+\boldsymbol{y}^T\boldsymbol{q}_3)(1+\boldsymbol{y}^T\boldsymbol{q}_{2,1})\\
&+\frac{29}{5}(1+\boldsymbol{y}^T\boldsymbol{q}_{3,1})(1+\boldsymbol{y}^T\boldsymbol{q}_2)(1+\boldsymbol{y}^T\boldsymbol{q}_{2,1})+\frac{11}{15}(1+\boldsymbol{y}^T\boldsymbol{q}_{2,3})(1+\boldsymbol{y}^T\boldsymbol{q}_2)(1+\boldsymbol{y}^T\boldsymbol{q}_{2,1})\Big).
\end{aligned}$$

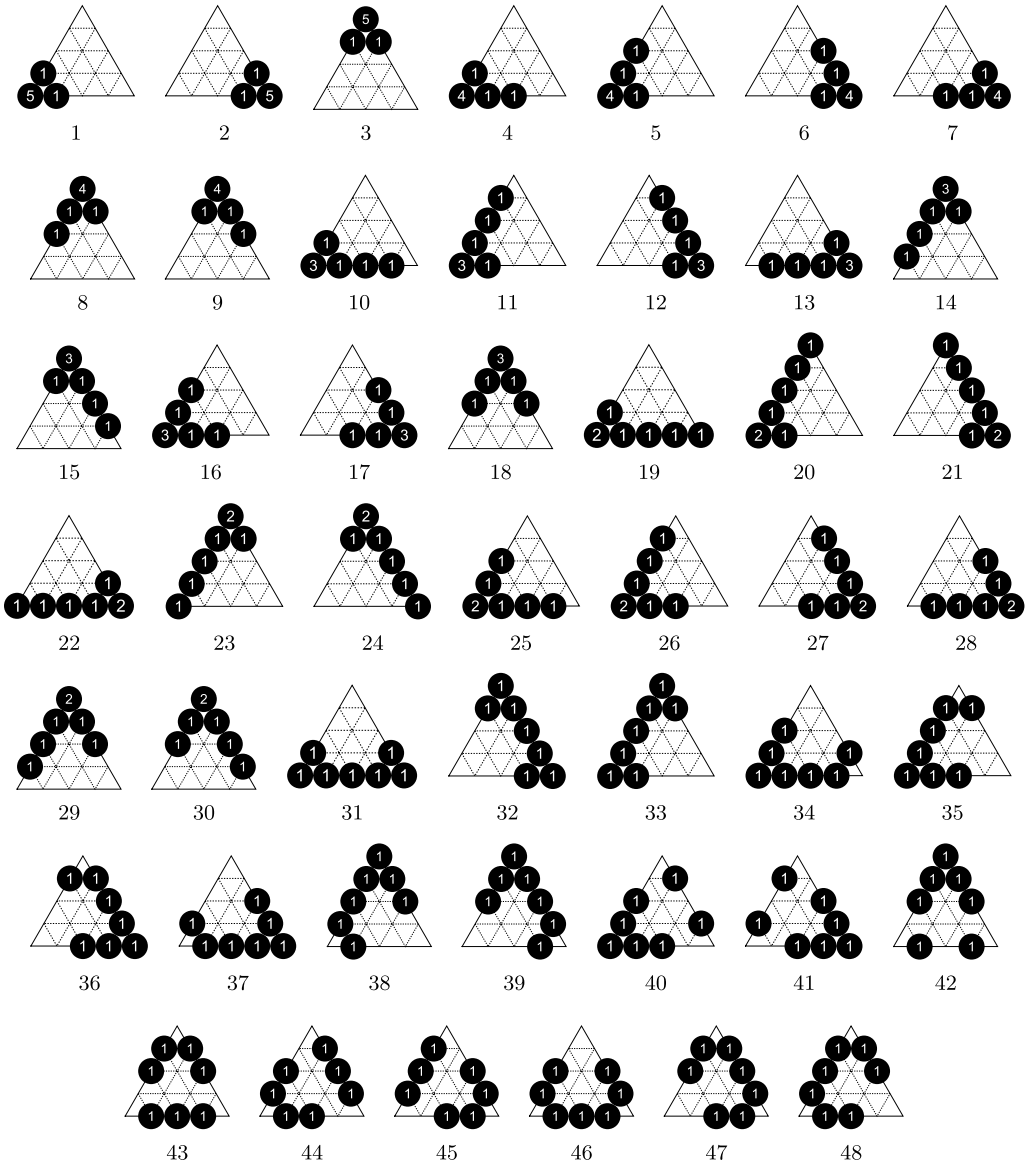

Fig. 8. Sequences of knots for a set of simplex spline basis functions for a subspace of $\mathbb{S}_4^3(\Delta_{\mathrm{WS}_4})$. Each black disc shows the position of a knot and the number inside indicates its multiplicity.

3.4. A proper subspace

As observed in Section 3.2, the domain points for the basis functions in (5) are not all distinct and this makes their use of limited interest in geometric modeling. We now provide a proper subspace of the space $\mathbb{S}_4^3(\Delta_{\mathrm{WS}_4})$, still containing $\mathbb{P}_4$, which can be equipped with a simplex spline basis whose elements enjoy distinct domain points.

We consider the subspace spanned by the simplex splines identified by the knot sequences in Fig. 8 and scaled to form a partition of unity. We denote these functions by

$$\widehat{\mathcal{B}} := \{\widehat{B}_1, \dots, \widehat{B}_{48}\}. \tag{21}$$

It can be directly checked that

$$\begin{aligned} &\widehat{B}_i = B_i, \quad i = 1, \dots, 39, \\ &\widehat{B}_{40} = B_{40} + B_{41}, \quad \widehat{B}_{41} = B_{42} + B_{43}, \quad \widehat{B}_{42} = B_{44} + B_{45}, \\ &\widehat{B}_i = B_{i+3}, \quad i = 43, \dots, 48. \end{aligned} \tag{22}$$

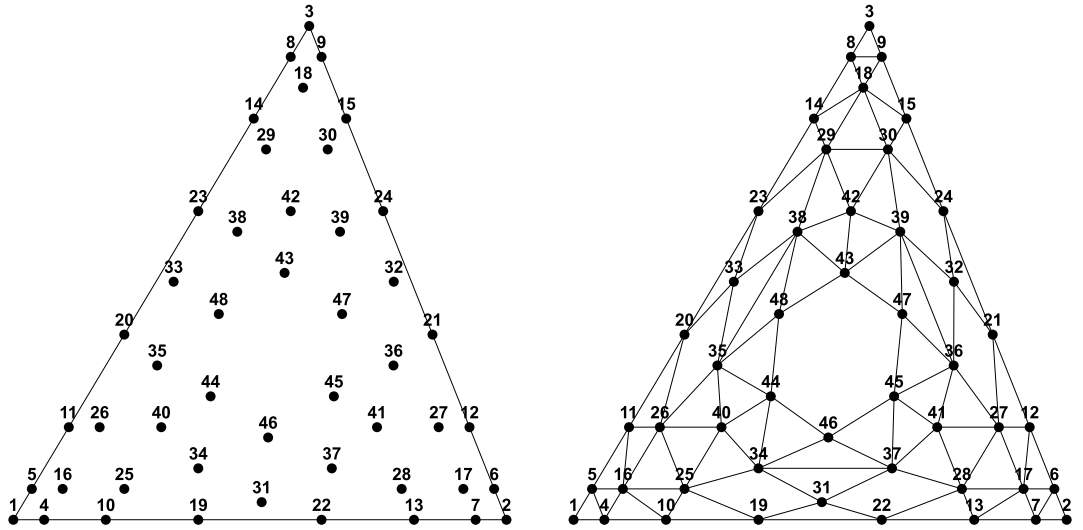

Fig. 9. Left: The domain points for the subspace $\widehat{\mathbb{S}}_4^3(\Delta_{\mathrm{WS}_4})$. Right: A possible control net configuration.

From (22) we easily deduce that the domain points $\hat{\boldsymbol{b}}_i^*$ associated with the new set of functions in (21) are

$$\begin{aligned} &\hat{\boldsymbol{b}}_i^* = \boldsymbol{b}_i^*, \quad i = 1, \dots, 39, \\ &\hat{\boldsymbol{b}}_{40}^* = \boldsymbol{b}_{40}^* = \boldsymbol{b}_{41}^*, \quad \hat{\boldsymbol{b}}_{41}^* = \boldsymbol{b}_{42}^* = \boldsymbol{b}_{43}^*, \quad \hat{\boldsymbol{b}}_{42}^* = \boldsymbol{b}_{44}^* = \boldsymbol{b}_{45}^*, \\ &\hat{\boldsymbol{b}}_i^* = \boldsymbol{b}_{i+3}^*, \quad i = 43, \dots, 48. \end{aligned} \tag{23}$$

These points are depicted in Fig. 9 (left) and a possible control net with triangular and hexagonal connectivity in Fig. 9 (right). Note that, contrarily to the domain points associated with the basis (5), the points in (23) are all distinct and therefore allow us to define a proper control net.

The distribution of the domain points in (23) makes the considered subspace particularly attractive from the geometric modeling point of view. The following result ensures that the subspace also contains all quartic polynomials and so can provide full approximation power.

Proposition 4. *Let* $\widehat{\mathbb{S}}_4^3(\Delta_{\mathrm{WS}_4})$ *be the subspace of* $\mathbb{S}_4^3(\Delta_{\mathrm{WS}_4})$ *spanned by the functions in* (21)*. Then,*

$$\mathbb{P}_4 \subset \widehat{\mathbb{S}}_4^3(\Delta_{\mathrm{WS}_4}).$$

Proof. The result follows from (22) and from the expressions of the dual polynomials given in Theorem 3 for $i = 40, 41, 42, 43, 44, 45$. □

4. C^3 quartic splines on general triangulations

In the previous section, we have provided a simplex spline basis for the space $\mathbb{S}_4^3(\Delta_{\mathrm{WS}_4})$ of C^3 quartic splines on the WS_4 split of a given triangle Δ. In this section, we discuss how the WS_4 split can be used as refinement strategy to locally construct C^3 quartic splines on general triangulations. Let $\mathcal{T}$ be a triangulation of a polygonal domain Ω and let $\mathcal{T}_{\mathrm{WS}_4}$ denote its refinement obtained by taking the WS_4 split of each triangle in $\mathcal{T}$.

4.1. C^3 quartic splines on $\mathcal{T}_{\mathrm{WS}_4}$

Let us consider the space of C^3 quartic splines on $\mathcal{T}_{\mathrm{WS}_4}$, i.e.,

$$\mathbb{S}_4^3(\mathcal{T}_{\mathrm{WS}_4}) := \{ s \in C^3(\Omega) : s_{|\tau} \in \mathbb{P}_4, \ \tau \text{ is polygon in } \mathcal{T}_{\mathrm{WS}_4} \}.$$

The unisolvency of the local Hermite interpolation problem stated in Corollary 2 implies that the dimension of the global space $\mathbb{S}_4^3(\mathcal{T}_{\mathrm{WS}_4})$ only depends on combinatorial properties of the triangulation. Indeed, for a given triangle Δ and any of its edges, say $\boldsymbol{p}_1\boldsymbol{p}_2$, the interpolation data (11)–(16) associated with points on the considered edge (namely $\boldsymbol{p}_1$, $\boldsymbol{q}_{3,1}$, $\boldsymbol{q}_3$, $\boldsymbol{q}_{3,2}$, and $\boldsymbol{p}_2$) completely characterize the values of the spline and its derivatives up to order three along the entire edge. More precisely, along this edge, any element of $\mathbb{S}_4^3(\Delta_{\mathrm{WS}_4})$ is a univariate C^3 quartic spline with break points at $\boldsymbol{p}_1$, $\boldsymbol{q}_{3,1}$, $\boldsymbol{q}_3$, $\boldsymbol{q}_{3,2}$, and $\boldsymbol{p}_2$. Therefore, it is uniquely determined by its values and derivatives (in the direction of the edge) up to order three at the two vertices $\boldsymbol{p}_1$ and $\boldsymbol{p}_2$. Similarly,

along the edge, the first, second, and third derivatives (in any direction) of the spline are univariate C^2 cubic, C^1 quadratic, and C^0 linear splines, respectively, with the same break points. The considered Hermite data also uniquely specify their values. Hence, we directly deduce that

$$\dim(\mathbb{S}_4^3(\mathcal{T}_{\mathrm{WS}_4})) = 10n_V + 6n_E + 3n_T, \tag{24}$$

where n_V, n_E, n_T are the number of vertices, edges, and triangles of $\mathcal{T}$, respectively; see also [31, Theorem 7.28].

Any spline function of $\mathbb{S}_4^3(\mathcal{T}_{\mathrm{WS}_4})$ can be locally constructed on each (macro-)triangle Δ of $\mathcal{T}$ via the Hermite data (used in Corollary 2), and the corresponding spline piece on Δ can be represented in the form (19). Conversely, any function, which is represented locally in the form (19) on each Δ of $\mathcal{T}$, is C^3 smooth over each Δ of $\mathcal{T}$ but not necessary C^3 smooth across the edges of $\mathcal{T}$. For this reason we refer to the basis in (5) as *local simplex spline basis* for the space $\mathbb{S}_4^3(\mathcal{T}_{\mathrm{WS}_4})$. Such a local basis plays the same role as Bernstein polynomials for spline spaces on triangulations that are not refined.

A global basis for the space $\mathbb{S}_4^3(\mathcal{T}_{\mathrm{WS}_4})$ can be constructed by using the technique of minimal determining sets [13], following the same line of arguments as in [15, Section 4.2]. However, paraphrasing [13, Section 5.8], such a global basis has mainly a theoretical interest. For computation in $\mathbb{S}_4^3(\mathcal{T}_{\mathrm{WS}_4})$, it is more convenient to work directly with the local representations provided by the basis in (5), rather than with the global basis for the full spline space. The smoothness relations between the local representations across the edges of the triangulation $\mathcal{T}$ are a crucial ingredient in the construction of minimal determining sets. In the next two sections, we will derive conditions on the local spline coefficients in (19) that ensure global smoothness across the edges of $\mathcal{T}$.

4.2. Global C^2 smoothness conditions

In this section, we seek conditions on the local spline coefficients in (19) to guarantee C^0, C^1, and C^2 smoothness across a common edge of two adjacent triangles of $\mathcal{T}$. In Section 4.3, we will address C^3 smoothness. To this end, we start by defining specific operators, similar to the ones in (7)–(9): $\varsigma_1, \dots, \varsigma_6$ are related to first derivatives at points on the edge $\boldsymbol{p}_1\boldsymbol{p}_2$,

$$\begin{aligned}
&\varsigma_1(f) := D_{\boldsymbol{p}_1\boldsymbol{p}_3} f(\boldsymbol{p}_1), \quad \varsigma_2(f) := D_{\boldsymbol{p}_1\boldsymbol{p}_2} f(\boldsymbol{p}_1), \quad \varsigma_3(f) := D_{\boldsymbol{p}_1\boldsymbol{p}_3} f(\boldsymbol{q}_3),\\
&\varsigma_4(f) := D_{\boldsymbol{p}_1\boldsymbol{p}_2} f(\boldsymbol{q}_3), \quad \varsigma_5(f) := D_{\boldsymbol{p}_1\boldsymbol{p}_3} f(\boldsymbol{p}_2), \quad \varsigma_6(f) := D_{\boldsymbol{p}_1\boldsymbol{p}_2} f(\boldsymbol{p}_2);
\end{aligned} \tag{25}$$

$\varsigma_7, \dots, \varsigma_{18}$ are related to second derivatives at points on the edge $\boldsymbol{p}_1\boldsymbol{p}_2$,

$$\begin{aligned}
&\varsigma_7(f) := D^2_{\boldsymbol{p}_1\boldsymbol{p}_3} f(\boldsymbol{p}_1), \quad \varsigma_8(f) := D_{\boldsymbol{p}_1\boldsymbol{p}_3} D_{\boldsymbol{p}_1\boldsymbol{p}_2} f(\boldsymbol{p}_1), \quad \varsigma_9(f) := D^2_{\boldsymbol{p}_1\boldsymbol{p}_2} f(\boldsymbol{p}_1),\\
&\varsigma_{10}(f) := D^2_{\boldsymbol{p}_1\boldsymbol{p}_3} f(\boldsymbol{q}_{3,1}), \quad \varsigma_{11}(f) := D_{\boldsymbol{p}_1\boldsymbol{p}_3} D_{\boldsymbol{p}_1\boldsymbol{p}_2} f(\boldsymbol{q}_{3,1}), \quad \varsigma_{12}(f) := D^2_{\boldsymbol{p}_1\boldsymbol{p}_2} f(\boldsymbol{q}_{3,1}),\\
&\varsigma_{13}(f) := D^2_{\boldsymbol{p}_1\boldsymbol{p}_3} f(\boldsymbol{q}_{3,2}), \quad \varsigma_{14}(f) := D_{\boldsymbol{p}_1\boldsymbol{p}_3} D_{\boldsymbol{p}_1\boldsymbol{p}_2} f(\boldsymbol{q}_{3,2}), \quad \varsigma_{15}(f) := D^2_{\boldsymbol{p}_1\boldsymbol{p}_2} f(\boldsymbol{q}_{3,2}),\\
&\varsigma_{16}(f) := D^2_{\boldsymbol{p}_1\boldsymbol{p}_3} f(\boldsymbol{p}_2), \quad \varsigma_{17}(f) := D_{\boldsymbol{p}_1\boldsymbol{p}_3} D_{\boldsymbol{p}_1\boldsymbol{p}_2} f(\boldsymbol{p}_2), \quad \varsigma_{18}(f) := D^2_{\boldsymbol{p}_1\boldsymbol{p}_2} f(\boldsymbol{p}_2);
\end{aligned} \tag{26}$$

and $\varsigma_{19}, \dots, \varsigma_{38}$ are related to third derivatives at points on the edge $\boldsymbol{p}_1\boldsymbol{p}_2$,

$$\begin{aligned}
&\varsigma_{19}(f) := D^3_{\boldsymbol{p}_1\boldsymbol{p}_3} f(\boldsymbol{p}_1), && \varsigma_{20}(f) := D^2_{\boldsymbol{p}_1\boldsymbol{p}_3} D_{\boldsymbol{p}_1\boldsymbol{p}_2} f(\boldsymbol{p}_1), && \varsigma_{21}(f) := D_{\boldsymbol{p}_1\boldsymbol{p}_3} D^2_{\boldsymbol{p}_1\boldsymbol{p}_2} f(\boldsymbol{p}_1),\\
&\varsigma_{22}(f) := D^3_{\boldsymbol{p}_1\boldsymbol{p}_2} f(\boldsymbol{p}_1), && \varsigma_{23}(f) := D^3_{\boldsymbol{p}_1\boldsymbol{p}_3} f(\boldsymbol{q}_{3,1}), && \varsigma_{24}(f) := D^2_{\boldsymbol{p}_1\boldsymbol{p}_3} D_{\boldsymbol{p}_1\boldsymbol{p}_2} f(\boldsymbol{q}_{3,1}),\\
&\varsigma_{25}(f) := D_{\boldsymbol{p}_1\boldsymbol{p}_3} D^2_{\boldsymbol{p}_1\boldsymbol{p}_2} f(\boldsymbol{q}_{3,1}), && \varsigma_{26}(f) := D^3_{\boldsymbol{p}_1\boldsymbol{p}_2} f(\boldsymbol{q}_{3,1}), && \varsigma_{27}(f) := D^3_{\boldsymbol{p}_1\boldsymbol{p}_3} f(\boldsymbol{q}_3),\\
&\varsigma_{28}(f) := D^2_{\boldsymbol{p}_1\boldsymbol{p}_3} D_{\boldsymbol{p}_1\boldsymbol{p}_2} f(\boldsymbol{q}_3), && \varsigma_{29}(f) := D_{\boldsymbol{p}_1\boldsymbol{p}_3} D^2_{\boldsymbol{p}_1\boldsymbol{p}_2} f(\boldsymbol{q}_3), && \varsigma_{30}(f) := D^3_{\boldsymbol{p}_1\boldsymbol{p}_2} f(\boldsymbol{q}_3),\\
&\varsigma_{31}(f) := D^3_{\boldsymbol{p}_1\boldsymbol{p}_3} f(\boldsymbol{q}_{3,2}), && \varsigma_{32}(f) := D^2_{\boldsymbol{p}_1\boldsymbol{p}_3} D_{\boldsymbol{p}_1\boldsymbol{p}_2} f(\boldsymbol{q}_{3,2}), && \varsigma_{33}(f) := D_{\boldsymbol{p}_1\boldsymbol{p}_3} D^2_{\boldsymbol{p}_1\boldsymbol{p}_2} f(\boldsymbol{q}_{3,2}),\\
&\varsigma_{34}(f) := D^3_{\boldsymbol{p}_1\boldsymbol{p}_2} f(\boldsymbol{q}_{3,2}), && \varsigma_{35}(f) := D^3_{\boldsymbol{p}_1\boldsymbol{p}_3} f(\boldsymbol{p}_2), && \varsigma_{36}(f) := D^2_{\boldsymbol{p}_1\boldsymbol{p}_3} D_{\boldsymbol{p}_1\boldsymbol{p}_2} f(\boldsymbol{p}_2),\\
&\varsigma_{37}(f) := D_{\boldsymbol{p}_1\boldsymbol{p}_3} D^2_{\boldsymbol{p}_1\boldsymbol{p}_2} f(\boldsymbol{p}_2), && \varsigma_{38}(f) := D^3_{\boldsymbol{p}_1\boldsymbol{p}_2} f(\boldsymbol{p}_2).
\end{aligned} \tag{27}$$

We apply them to all the basis functions in (5); the resulting values are collected in Tables 6–8 in the appendix.

Theorem 5. *Suppose the triangles $\Delta^L := \langle \boldsymbol{p}_1, \boldsymbol{p}_2, \boldsymbol{p}_3 \rangle$ and $\Delta^R := \langle \boldsymbol{p}_1, \boldsymbol{p}_2, \boldsymbol{p}_4 \rangle$ share the common edge with vertices $\boldsymbol{p}_1, \boldsymbol{p}_2$, and let*

$$\boldsymbol{p}_4 = \eta_1 \boldsymbol{p}_1 + \eta_2 \boldsymbol{p}_2 + \eta_3 \boldsymbol{p}_3, \quad \eta_1 + \eta_2 + \eta_3 = 1. \tag{28}$$

Let $\{B_i^L,\ i = 1, \dots, 51\}$ and $\{B_i^R,\ i = 1, \dots, 51\}$ be the scaled simplex spline basis defined by the knot sequences in Fig. 5 on Δ^L and Δ^R, respectively. We assume the numbering of the basis functions in agreement with Fig. 5. Let us consider the spline functions

$$s^L := \sum_{i=1}^{51} b_i^L B_i^L, \quad s^R := \sum_{i=1}^{51} b_i^R B_i^R.$$

We have

- s^L, s^R *join* C^0 *across the common edge if and only if*

$$b_i^R = b_i^L, \quad i = 1,2,4,7,10,13,19,22; \tag{29}$$

- s^L, s^R *join* C^1 *across the common edge if and only if they join* C^0 *and in addition*

$$\begin{aligned}
b_5^R &= \eta_1 b_1^L + \eta_2 b_4^L + \eta_3 b_5^L,\\
b_{16}^R &= \Big(\eta_1 + \frac{\eta_2}{2}\Big) b_4^L + \frac{\eta_2}{2} b_{10}^L + \eta_3 b_{16}^L,\\
b_{25}^R &= \Big(\eta_1 + \frac{2}{3}\eta_2\Big) b_{10}^L + \frac{\eta_2}{3} b_{19}^L + \eta_3 b_{25}^L,\\
b_{31}^R &= \Big(\frac{4}{7}\eta_1 + \frac{3}{7}\eta_2\Big) b_{19}^L + \Big(\frac{3}{7}\eta_1 + \frac{4}{7}\eta_2\Big) b_{22}^L + \eta_3 b_{31}^L,\\
b_{28}^R &= \Big(\eta_2 + \frac{2}{3}\eta_1\Big) b_{13}^L + \frac{\eta_1}{3} b_{22}^L + \eta_3 b_{28}^L,\\
b_{17}^R &= \Big(\eta_2 + \frac{\eta_1}{2}\Big) b_7^L + \frac{\eta_1}{2} b_{13}^L + \eta_3 b_{17}^L,\\
b_6^R &= \eta_1 b_7^L + \eta_2 b_2^L + \eta_3 b_6^L;
\end{aligned} \tag{30}$$

- s^L, s^R *join* C^2 *across the common edge if and only if they join* C^1 *and in addition*

$$\begin{aligned}
b_{11}^R &= \eta_1(2\eta_1 - 1) b_1^L + \eta_2(3\eta_1 - \eta_3) b_4^L + \eta_3(3\eta_1 - \eta_2) b_5^L + \eta_2^2 b_{10}^L + \eta_3^2 b_{11}^L + 4\eta_3\eta_2 b_{16}^L,\\
b_{26}^R &= \frac{1}{2}(2\eta_1 + \eta_2)(\eta_1 - \eta_3) b_4^L + \frac{\eta_2}{6}(9\eta_1 + 4\eta_2 - 3\eta_3) b_{10}^L + \eta_3(3\eta_1 + \eta_2) b_{16}^L + \frac{1}{3}\eta_2^2 b_{19}^L + 2\eta_3\eta_2 b_{25}^L + \eta_3^2 b_{26}^L,\\
b_{34}^R &= \frac{1}{27}(2\eta_2 + 3\eta_1)(\eta_2 + 3\eta_1 - 3\eta_3) b_{10}^L + \frac{1}{54}\big(12\eta_1(2\eta_2 + 3) + \eta_2(17\eta_2 + 21)\big) b_{19}^L\\
&\quad + \frac{1}{18}(3\eta_1 + 4\eta_2)(\eta_2 - 3\eta_3) b_{22}^L + \frac{\eta_3}{9}(9\eta_1 + 5\eta_2) b_{25}^L + \frac{7}{18}\eta_3(3\eta_1 + 5\eta_2) b_{31}^L + \eta_3^2 b_{34}^L,\\
b_{37}^R &= \frac{1}{27}(2\eta_1 + 3\eta_2)(\eta_1 + 3\eta_2 - 3\eta_3) b_{13}^L + \frac{1}{54}\big(12\eta_2(2\eta_1 + 3) + \eta_1(17\eta_1 + 21)\big) b_{22}^L\\
&\quad + \frac{1}{18}(3\eta_2 + 4\eta_1)(\eta_1 - 3\eta_3) b_{19}^L + \frac{\eta_3}{9}(9\eta_2 + 5\eta_1) b_{28}^L + \frac{7}{18}\eta_3(3\eta_2 + 5\eta_1) b_{31}^L + \eta_3^2 b_{37}^L,\\
b_{27}^R &= \frac{1}{2}(2\eta_2 + \eta_1)(\eta_2 - \eta_3) b_7^L + \frac{\eta_1}{6}(9\eta_2 + 4\eta_1 - 3\eta_3) b_{13}^L + \eta_3(3\eta_2 + \eta_1) b_{17}^L + \frac{1}{3}\eta_1^2 b_{22}^L + 2\eta_3\eta_1 b_{28}^L + \eta_3^2 b_{27}^L,\\
b_{12}^R &= \eta_2(2\eta_2 - 1) b_2^L + \eta_1(3\eta_2 - \eta_3) b_7^L + \eta_3(3\eta_2 - \eta_1) b_6^L + \eta_1^2 b_{13}^L + \eta_3^2 b_{12}^L + 4\eta_3\eta_1 b_{17}^L.
\end{aligned} \tag{31}$$

Proof. First, we show that the conditions of (29) lead to C^0 smoothness across the common edge $\boldsymbol{p}_1\boldsymbol{p}_2$. The restrictions onto this edge of the two functions s^L and s^R are univariate C^3 quartic splines with (interior) knots at the points $\boldsymbol{q}_{3,1}$, $\boldsymbol{q}_3$, and $\boldsymbol{q}_{3,2}$. In particular, considering the corresponding basis functions $\{B_i^L,\ i = 1,\dots,51\}$ and $\{B_i^R,\ i = 1,\dots,51\}$, the only elements that are nonzero along the edge are

$$(B_i^R)_{|\boldsymbol{p}_1\boldsymbol{p}_2} = (B_i^L)_{|\boldsymbol{p}_1\boldsymbol{p}_2}, \quad i = 1,2,4,7,10,13,19,22,$$

and these are nothing but the univariate quartic B-splines on the knot sequence specified by $\{\boldsymbol{p}_1,\boldsymbol{p}_1,\boldsymbol{p}_1,\boldsymbol{p}_1,\boldsymbol{p}_1,\boldsymbol{q}_{3,1},\boldsymbol{q}_3,\boldsymbol{q}_{3,2},\boldsymbol{p}_2,\boldsymbol{p}_2,\boldsymbol{p}_2,\boldsymbol{p}_2,\boldsymbol{p}_2\}$. They are linearly independent and so C^0 smoothness is equivalent to agreement of the corresponding coefficients. This proves (29).

Next, we consider C^1 smoothness across the common edge. It suffices to prove that along the edge $\boldsymbol{p}_1\boldsymbol{p}_2$ the functions $D_{\boldsymbol{p}_1\boldsymbol{p}_3} s^L$ and $D_{\boldsymbol{p}_1\boldsymbol{p}_3} s^R$ agree. These functions are univariate C^2 cubic splines with (interior) knots at the points $\boldsymbol{q}_{3,1}$, $\boldsymbol{q}_3$, and $\boldsymbol{q}_{3,2}$. Therefore, each of them is uniquely determined by its value and its first and second derivative at the two endpoints of the edge and by the value at the midpoint $\boldsymbol{q}_3$. From (28) we know that

$$\boldsymbol{p}_1\boldsymbol{p}_3 = \frac{1}{\eta_3}\boldsymbol{p}_1\boldsymbol{p}_4 - \frac{\eta_2}{\eta_3}\boldsymbol{p}_1\boldsymbol{p}_2,$$

so that

$$D_{\boldsymbol{p}_1\boldsymbol{p}_3} = \frac{1}{\eta_3} D_{\boldsymbol{p}_1\boldsymbol{p}_4} - \frac{\eta_2}{\eta_3} D_{\boldsymbol{p}_1\boldsymbol{p}_2}.$$

By employing the values in Table 6 we get

$$\begin{aligned}
D_{\boldsymbol{p}_1\boldsymbol{p}_3} s^L(\boldsymbol{p}_1) &= -16 b_1^L + 16 b_5^L,\\
D_{\boldsymbol{p}_1\boldsymbol{p}_3} s^R(\boldsymbol{p}_1) &= \frac{1}{\eta_3}(-16 b_1^R + 16 b_5^R) - \frac{\eta_2}{\eta_3}(-16 b_1^R + 16 b_4^R).
\end{aligned}$$

With the aid of the C^0 smoothness conditions, equating the above expressions results in the first condition of (30). With a similar line of arguments, we can show the remaining six conditions of (30).

Finally, we outline the proof for C^2 smoothness. Assume s^L and s^R join C^1 across the common edge $\boldsymbol{p}_1\boldsymbol{p}_2$. To prove C^2 smoothness across the same edge, it suffices to prove that along $\boldsymbol{p}_1\boldsymbol{p}_2$ the functions $D^2_{\boldsymbol{p}_1\boldsymbol{p}_3}s^L$ and $D^2_{\boldsymbol{p}_1\boldsymbol{p}_3}s^R$ agree. Along the edge $\boldsymbol{p}_1\boldsymbol{p}_2$, the above functions are univariate C^1 quadratic splines with (interior) knots at the points $\boldsymbol{q}_{3,1}$, $\boldsymbol{q}_3$, and $\boldsymbol{q}_{3,2}$. Therefore, each of them is uniquely determined by its value and its first derivative at the two endpoints of the edge and by the value at the points $\boldsymbol{q}_{3,1}$ and $\boldsymbol{q}_{3,2}$. From (28) we know that

$$D^2_{\boldsymbol{p}_1\boldsymbol{p}_3} = \Big(\frac{1}{\eta_3}D_{\boldsymbol{p}_1\boldsymbol{p}_4} - \frac{\eta_2}{\eta_3}D_{\boldsymbol{p}_1\boldsymbol{p}_2}\Big)^2.$$

By employing the values in Table 6 in the appendix, a direct computation gives

$$D^2_{\boldsymbol{p}_1\boldsymbol{p}_3}s^L(\boldsymbol{p}_1) = 192b^L_1 - 288b^L_5 + 96b^L_{11},$$

$$D^2_{\boldsymbol{p}_1\boldsymbol{p}_3}s^R(\boldsymbol{p}_1) = \frac{1}{\eta_3^2}(192b^R_1 - 288b^R_5 + 96b^R_{11}) - \frac{2\eta_2}{\eta_3^2}(192b^R_1 - 192b^R_4 - 192b^R_5 + 192b^R_{16}) + \frac{\eta_2^2}{\eta_3^2}(192b^R_1 - 288b^R_4 + 96b^R_{10}).$$

By equating these expressions and taking into account the C^1 smoothness conditions, we get the first equation in (31). With a similar line of arguments, we can show the remaining five relations in (31). □

Some remarks are in order.

Remark 6. The Cartesian coordinates of the domain points $\boldsymbol{b}^{*L}_i$ and $\boldsymbol{b}^{*R}_i$, $i = 1,\dots,51$ in two adjacent triangles Δ^L and Δ^R satisfy conditions (29)–(31) across the common edge because they are the coefficients related to the two local simplex spline bases of the smooth functions $f_1(x,y) := x$ and $f_2(x,y) := y$. This allows us to give a nice geometric interpretation to the above mentioned smoothness conditions in terms of control points in a full analogy with the interpretation of smoothness conditions for the Bernstein–Bézier representation. For C^0 smoothness, only the eight pairs of control points associated with the common edge are involved and the elements of each pair must coincide, i.e.,

$$(\boldsymbol{b}^{*R}_i, b^R_i) = (\boldsymbol{b}^{*L}_i, b^L_i), \quad i = 1,2,4,7,10,13,19,22.$$

For C^1 smoothness, there are seven sets of four control points along the common edge that must be all pairwise coplanar, i.e.,

$$(\boldsymbol{b}^{*R}_5, b^R_5) = \eta_1(\boldsymbol{b}^{*L}_1, b^L_1) + \eta_2(\boldsymbol{b}^{*L}_4, b^L_4) + \eta_3(\boldsymbol{b}^{*L}_5, b^L_5),$$
$$(\boldsymbol{b}^{*R}_{16}, b^R_{16}) = \Big(\eta_1 + \frac{\eta_2}{2}\Big)(\boldsymbol{b}^{*L}_4, b^L_4) + \frac{\eta_2}{2}(\boldsymbol{b}^{*L}_{10}, b^L_{10}) + \eta_3(\boldsymbol{b}^{*L}_{16}, b^L_{16}),$$
$$(\boldsymbol{b}^{*R}_{25}, b^R_{25}) = \Big(\eta_1 + \frac{2}{3}\eta_2\Big)(\boldsymbol{b}^{*L}_{10}, b^L_{10}) + \frac{\eta_2}{3}(\boldsymbol{b}^{*L}_{19}, b^L_{19}) + \eta_3(\boldsymbol{b}^{*L}_{25}, b^L_{25}),$$
$$(\boldsymbol{b}^{*R}_{31}, b^R_{31}) = \Big(\frac{4}{7}\eta_1 + \frac{3}{7}\eta_2\Big)(\boldsymbol{b}^{*L}_{19}, b^L_{19}) + \Big(\frac{3}{7}\eta_1 + \frac{4}{7}\eta_2\Big)(\boldsymbol{b}^{*L}_{22}, b^L_{22}) + \eta_3(\boldsymbol{b}^{*L}_{31}, b^L_{31}),$$
$$(\boldsymbol{b}^{*R}_{28}, b^R_{28}) = \Big(\eta_2 + \frac{2}{3}\eta_1\Big)(\boldsymbol{b}^{*L}_{13}, b^L_{13}) + \frac{\eta_1}{3}(\boldsymbol{b}^{*L}_{22}, b^L_{22}) + \eta_3(\boldsymbol{b}^{*L}_{28}, b^L_{28}),$$
$$(\boldsymbol{b}^{*R}_{17}, b^R_{17}) = \Big(\eta_2 + \frac{\eta_1}{2}\Big)(\boldsymbol{b}^{*L}_7, b^L_7) + \frac{\eta_1}{2}(\boldsymbol{b}^{*L}_{13}, b^L_{13}) + \eta_3(\boldsymbol{b}^{*L}_{17}, b^L_{17}),$$
$$(\boldsymbol{b}^{*R}_6, b^R_6) = \eta_1(\boldsymbol{b}^{*L}_7, b^L_7) + \eta_2(\boldsymbol{b}^{*L}_2, b^L_2) + \eta_3(\boldsymbol{b}^{*L}_6, b^L_6);$$

see Fig. 10 for an illustration. Finally, also the C^2 smoothness conditions show a similarity with the C^2 join of two adjacent triangular Bernstein–Bézier patches; see [12, Example 2]. There are six sets of seven control points that must belong (separately) to a quadratic surface. For the sake of brevity we omit the equations that can be immediately obtained from (31).

Remark 7. Since the smoothness conditions provided in Theorem 5 do not involve the functions $\{B_i,\ i = 40,\dots,51\}$, the same relations also hold true for the subspace $\widehat{\mathbb{S}}^3_4(\Delta_{\mathrm{WS}_4})$ defined in Section 3.4.

4.3. Global C^3 smoothness conditions

The basis functions B_i, $i = 40,\dots,48$ and $i = 49,50,51$, can be associated with the degrees of freedom corresponding to third derivatives related to the edges of Δ (i.e., those used by the linear operators ρ_i, $i = 40,\dots,48$) and to function values at interior points (i.e., those used by the linear operators ρ_i, $i = 49,50,51$), however, they do not allow for a complete separation of these degrees of freedom. This can be understood by looking at the structure of the Hermite collocation matrix which is block triangular but not triangular in the part containing the last 11 rows/columns; see Tables 3–5 in the appendix. Unfortunately, this prevents the possibility of obtaining elegant localized conditions on the local spline coefficients in (19) for C^3 smoothness across the edges of $\mathcal{T}$.

Inspired by the approach in [15, Section 3.4], we consider an alternative local basis for $\mathbb{S}^3_4(\Delta_{\mathrm{WS}_4})$ to achieve more practical C^3 smoothness conditions. We denote this basis by

$$\widetilde{\mathcal{B}} := \{\widetilde{B}_1,\dots,\widetilde{B}_{51}\}. \tag{32}$$

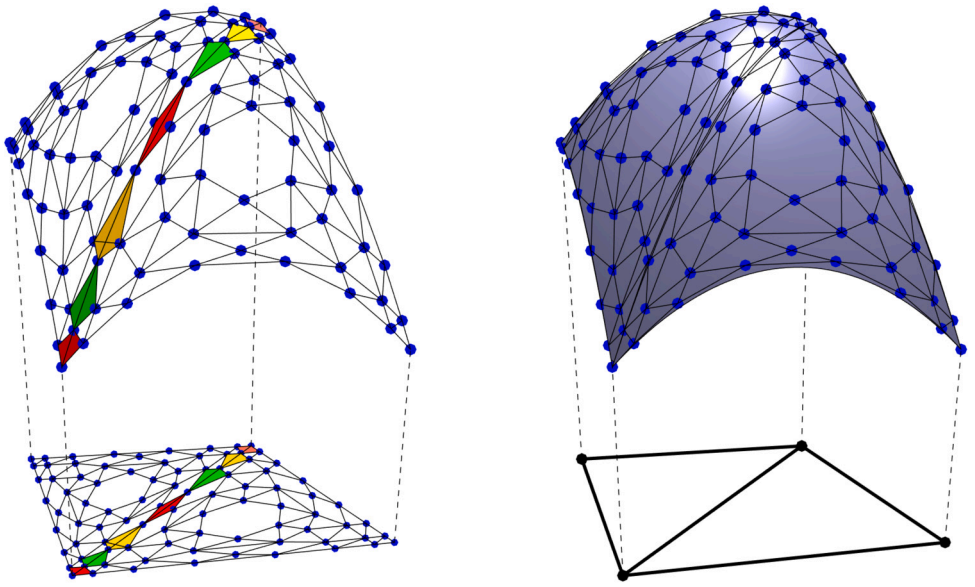

Fig. 10. A C^1 spline surface on two adjacent domain triangles. The 7 pairs of triangles in the control nets that must be coplanar according to the smoothness conditions are colored.

The functions in (32) are computed as

$$\widetilde{B}_i = B_i, \quad i = 1, \dots, 33,$$

and

$$(\widetilde{B}_{34}, \dots, \widetilde{B}_{51})^T = C\,(B_{34}, \dots, B_{51})^T,$$

where C is the conversion matrix specified in Table 2.

Theorem 8. *The functions* $\{\widetilde{B}_1, \dots, \widetilde{B}_{51}\}$ *in* (32) *form a partition of unity basis for the space* $\mathbb{S}_4^3(\Delta_{\mathrm{WS}_4})$. *Moreover, for any given direction, the third derivative in that direction vanishes*

a) *along the edge* $\boldsymbol{p}_1\boldsymbol{p}_2$ *for* $\widetilde{B}_{35}$, $\widetilde{B}_{36}$, $\widetilde{B}_{41}$, $\widetilde{B}_{42}$, $\widetilde{B}_{49}$;
b) *along the edge* $\boldsymbol{p}_2\boldsymbol{p}_3$ *for* $\widetilde{B}_{37}$, $\widetilde{B}_{38}$, $\widetilde{B}_{43}$, $\widetilde{B}_{44}$, $\widetilde{B}_{50}$;
c) *along the edge* $\boldsymbol{p}_1\boldsymbol{p}_3$ *for* $\widetilde{B}_{34}$, $\widetilde{B}_{39}$, $\widetilde{B}_{40}$, $\widetilde{B}_{45}$, $\widetilde{B}_{51}$.

Proof. Since the conversion matrix in Table 2 is nonsingular and each of its columns sum up to one, the functions in (32) inherit the properties of linear independence and partition of unity from the basis elements in (5); see Theorem 1.

Regarding the property of vanishing third derivatives, let us focus on the first case a). From the smoothness property of simplex splines it follows that the functions B_{35}, B_{36}, B_{40}, B_{41}, B_{42}, B_{43}, B_{46}, B_{49} are C^2 smooth across the edge $\boldsymbol{p}_1\boldsymbol{p}_2$ (see Fig. 5), thus they vanish with all their derivatives up to order two along the edge. By construction, this property carries over to the functions $\widetilde{B}_{35}$, $\widetilde{B}_{36}$, $\widetilde{B}_{41}$, $\widetilde{B}_{42}$, $\widetilde{B}_{49}$. Moreover, along the same edge, the third derivative in any direction of these functions is a univariate C^0 linear spline with break points at $\boldsymbol{p}_1$, $\boldsymbol{q}_{3,1}$, $\boldsymbol{q}_3$, $\boldsymbol{q}_{3,2}$, $\boldsymbol{p}_2$. Now, let us consider the function $\widetilde{B}_{35}$. Taking into account the supports of B_{35}, B_{40}, and B_{41}, a direct inspection of the values in Table 2 and Tables 4,5 in the appendix shows that

$$D^3_{\boldsymbol{q}_{3,1}\boldsymbol{p}_3}\widetilde{B}_{35}(\boldsymbol{p}_1) = D^3_{\boldsymbol{q}_{3,1}\boldsymbol{p}_3}\widetilde{B}_{35}(\boldsymbol{q}_{3,1}) = D^3_{\boldsymbol{q}_{3,1}\boldsymbol{p}_3}\widetilde{B}_{35}(\boldsymbol{q}_3) = D^3_{\boldsymbol{q}_{3,1}\boldsymbol{p}_3}\widetilde{B}_{35}(\boldsymbol{q}_{3,2}) = D^3_{\boldsymbol{q}_{3,1}\boldsymbol{p}_3}\widetilde{B}_{35}(\boldsymbol{p}_2) = 0.$$

Therefore, $D^3_{\boldsymbol{q}_{3,1}\boldsymbol{p}_3}\widetilde{B}_{35}$ vanishes along $\boldsymbol{p}_1\boldsymbol{p}_2$. Since we already know that all the derivatives of $\widetilde{B}_{35}$ vanish up to order two along $\boldsymbol{p}_1\boldsymbol{p}_2$, this implies that all third derivatives (in any direction) of $\widetilde{B}_{35}$ also vanish along $\boldsymbol{p}_1\boldsymbol{p}_2$. With the same line of arguments, the stated results for the other functions and the other derivative cases can be obtained as well. □

When representing spline functions on two adjacent macro-triangles sharing a common edge, say $\boldsymbol{p}_1\boldsymbol{p}_2$, in terms of the new basis (32), the C^2 smoothness conditions remain the same as given in Theorem 5. Indeed, any derivative up to the second order in any direction along $\boldsymbol{p}_1\boldsymbol{p}_2$ agrees for B_i and $\widetilde{B}_i$, $i = 1, \dots, 51$. On the other hand, the representation in the basis (32) allows us to derive simpler C^3 smoothness conditions.

Table 2
Conversion matrix between $\{B_{34},\dots,B_{51}\}$ and $\{\widetilde{B}_{34},\dots,\widetilde{B}_{51}\}$.

	B_{34}	B_{35}	B_{36}	B_{37}	B_{38}	B_{39}	B_{40}	B_{41}	B_{42}	B_{43}	B_{44}	B_{45}	B_{46}	B_{47}	B_{48}	B_{49}	B_{50}	B_{51}
$\widetilde{B}_{34}$	1	0	0	0	0	0	$-\frac{3}{4}$	$-\frac{1}{4}$	0	0	0	0	0	0	0	0	0	0
$\widetilde{B}_{35}$	0	1	0	0	0	0	$-\frac{1}{4}$	$-\frac{3}{4}$	0	0	0	0	0	0	0	0	0	0
$\widetilde{B}_{36}$	0	0	1	0	0	0	0	0	$-\frac{3}{4}$	$-\frac{1}{4}$	0	0	0	0	0	0	0	0
$\widetilde{B}_{37}$	0	0	0	1	0	0	0	0	$-\frac{1}{4}$	$-\frac{3}{4}$	0	0	0	0	0	0	0	0
$\widetilde{B}_{38}$	0	0	0	0	1	0	0	0	0	0	$-\frac{3}{4}$	$-\frac{1}{4}$	0	0	0	0	0	0
$\widetilde{B}_{39}$	0	0	0	0	0	1	0	0	0	0	$-\frac{1}{4}$	$-\frac{3}{4}$	0	0	0	0	0	0
$\widetilde{B}_{40}$	0	0	0	0	0	0	3	−1	0	0	0	0	0	0	0	0	0	0
$\widetilde{B}_{41}$	0	0	0	0	0	0	−1	3	0	0	0	0	0	0	0	0	0	0
$\widetilde{B}_{42}$	0	0	0	0	0	0	0	0	3	−1	0	0	0	0	0	0	0	0
$\widetilde{B}_{43}$	0	0	0	0	0	0	0	0	−1	3	0	0	0	0	0	0	0	0
$\widetilde{B}_{44}$	0	0	0	0	0	0	0	0	0	0	3	−1	0	0	0	0	0	0
$\widetilde{B}_{45}$	0	0	0	0	0	0	0	0	0	0	−1	3	0	0	0	0	0	0
$\widetilde{B}_{46}$	0	0	0	0	0	0	0	0	0	0	0	0	16	0	0	0	0	0
$\widetilde{B}_{47}$	0	0	0	0	0	0	0	0	0	0	0	0	0	16	0	0	0	0
$\widetilde{B}_{48}$	0	0	0	0	0	0	0	0	0	0	0	0	0	0	16	0	0	0
$\widetilde{B}_{49}$	0	0	0	0	0	0	0	0	0	0	0	0	−15	0	0	1	0	0
$\widetilde{B}_{50}$	0	0	0	0	0	0	0	0	0	0	0	0	0	−15	0	0	1	0
$\widetilde{B}_{51}$	0	0	0	0	0	0	0	0	0	0	0	0	0	0	−15	0	0	1

Theorem 9. *Consider the same assumptions as in Theorem 5. Let* $\{\widetilde{B}_i^L,\ i=1,\dots,51\}$ *and* $\{\widetilde{B}_i^R,\ i=1,\dots,51\}$ *be the spline bases as in* (32) *on* Δ^L *and* Δ^R*, respectively. Then, the spline functions*

$$s^L := \sum_{i=1}^{51} b_i^L B_i^L = \sum_{i=1}^{33} b_i^L B_i^L + \sum_{i=34}^{51} \tilde{b}_i^L \widetilde{B}_i^L$$

and

$$s^R := \sum_{i=1}^{51} b_i^R B_i^R = \sum_{i=1}^{33} b_i^R B_i^R + \sum_{i=34}^{51} \tilde{b}_i^R \widetilde{B}_i^R$$

join C^3 *across the common edge if and only if they join* C^2 *and in addition*

$$\begin{aligned} b_{20}^R &= \eta_1(2\eta_1-1)(3\eta_1-2)b_1^L + \frac{\eta_3}{2}(21\eta_1^2-12\eta_1\eta_2+3\eta_2^2-9\eta_1+\eta_2)b_5^L + \frac{\eta_2}{2}(36\eta_1^2+18\eta_1\eta_2+3\eta_2^2-28\eta_1-7\eta_2+4)b_4^L \\ &\quad + \frac{1}{2}\eta_3^2(11\eta_1-7\eta_2)b_{11}^L + \frac{1}{2}\eta_2^2(11\eta_1-7\eta_3)b_{10}^L + \eta_2\eta_3(27\eta_1-5)b_{16}^L + \eta_3^3 b_{20}^L + \eta_2^3 b_{19}^L + 9\eta_2\eta_3^2 b_{26}^L + 9\eta_2^2\eta_3 b_{25}^L, \end{aligned} \tag{33}$$

and

$$\begin{aligned} b_{21}^R &= \eta_2(2\eta_2-1)(3\eta_2-2)b_2^L + \frac{\eta_3}{2}(21\eta_2^2-12\eta_1\eta_2+3\eta_1^2-9\eta_2+\eta_1)b_6^L + \frac{\eta_1}{2}(36\eta_2^2+18\eta_1\eta_2+3\eta_1^2-28\eta_2-7\eta_1+4)b_7^L \\ &\quad + \frac{1}{2}\eta_3^2(11\eta_2-7\eta_1)b_{12}^L + \frac{1}{2}\eta_1^2(11\eta_2-7\eta_3)b_{13}^L + \eta_1\eta_3(27\eta_2-5)b_{17}^L + \eta_3^3 b_{21}^L + \eta_1^3 b_{22}^L + 9\eta_1\eta_3^2 b_{27}^L + 9\eta_1^2\eta_3 b_{28}^L, \end{aligned} \tag{34}$$

and

$$\begin{aligned} \tilde{b}_{40}^R &= \frac{1}{32}(2\eta_1+\eta_2)(\eta_1-\eta_3)(6\eta_1+3\eta_2-4)b_4^L + \Big(-\frac{23}{72}\eta_2 + \frac{71}{864}\eta_2^2 + \frac{21}{16}\eta_1\eta_2^2 + \frac{65}{72}\eta_1\eta_2 + \frac{9}{8}\eta_1^2\eta_2 + \frac{4}{3}\eta_1^2 - \frac{2}{3}\eta_1 + \frac{37}{96}\eta_2^3\Big)b_{10}^L \\ &\quad + \frac{\eta_3}{16}(21\eta_1^2+15\eta_1\eta_2+3\eta_2^2-9\eta_1-4\eta_2)b_{16}^L + \Big(-\frac{19}{288}\eta_2 + \frac{209}{432}\eta_2^2 + \frac{3}{8}\eta_2^2\eta_1 + \frac{8}{9}\eta_2\eta_1 + \frac{5}{24}\eta_1 + \frac{23}{96}\eta_2^3\Big)b_{19}^L \\ &\quad + \frac{1}{288}(3\eta_1+4\eta_2)(\eta_2-3\eta_3)(36\eta_2+27\eta_1-22)b_{22}^L + \frac{\eta_3}{144}(108\eta_2^2+243\eta_2\eta_1+115\eta_2+288\eta_1)b_{25}^L \\ &\quad + \frac{1}{16}\eta_3^2(11\eta_1+2\eta_2)b_{26}^L + \frac{7}{288}\eta_3(81\eta_1^2+243\eta_1\eta_2+189\eta_2^2-66\eta_1-83\eta_2)b_{31}^L + \frac{1}{16}\eta_3^2(32\eta_1+59\eta_2)\tilde{b}_{34}^L + \eta_3^3\tilde{b}_{40}^L, \end{aligned} \tag{35}$$

and

$$\begin{aligned} \tilde{b}_{43}^R &= \frac{1}{32}(2\eta_2+\eta_1)(\eta_2-\eta_3)(6\eta_2+3\eta_1-4)b_7^L + \Big(-\frac{23}{72}\eta_1 + \frac{71}{864}\eta_1^2 + \frac{21}{16}\eta_2\eta_1^2 + \frac{65}{72}\eta_2\eta_1 + \frac{9}{8}\eta_2^2\eta_1 + \frac{4}{3}\eta_2^2 - \frac{2}{3}\eta_2 + \frac{37}{96}\eta_1^3\Big)b_{13}^L \\ &\quad + \frac{\eta_3}{16}(21\eta_2^2+15\eta_2\eta_1+3\eta_1^2-9\eta_2-4\eta_1)b_{17}^L + \Big(-\frac{19}{288}\eta_1 + \frac{209}{432}\eta_1^2 + \frac{3}{8}\eta_1^2\eta_2 + \frac{8}{9}\eta_1\eta_2 + \frac{5}{24}\eta_2 + \frac{23}{96}\eta_1^3\Big)b_{22}^L \\ &\quad + \frac{1}{288}(3\eta_2+4\eta_1)(\eta_1-3\eta_3)(36\eta_1+27\eta_2-22)b_{19}^L + \frac{\eta_3}{144}(108\eta_1^2+243\eta_1\eta_2+115\eta_1+288\eta_2)b_{28}^L \\ &\quad + \frac{1}{16}\eta_3^2(11\eta_2+2\eta_1)b_{27}^L + \frac{7}{288}\eta_3(81\eta_2^2+243\eta_2\eta_1+189\eta_1^2-66\eta_2-83\eta_1)b_{31}^L + \frac{1}{16}\eta_3^2(32\eta_2+59\eta_1)\tilde{b}_{37}^L + \eta_3^3\tilde{b}_{43}^L, \end{aligned} \tag{36}$$

and

$$
\begin{aligned}
\tilde{b}^R_{46} = {} & \frac{1}{36}(2\eta_2+3\eta_1)(\eta_2+3\eta_3)(4\eta_3-2\eta_1-1)b^L_{10} + \frac{1}{36}(2\eta_1+3\eta_2)(\eta_1+3\eta_3)(4\eta_3-2\eta_2-1)b^L_{13} \\
& + \Big(3\eta_1^2 - \frac{2}{3}\eta_1^3 - \frac{7}{8}\eta_2 + \frac{5}{8}\eta_2^2 + 3\eta_1\eta_2 + \eta_1\eta_2^2 - \frac{3}{2}\eta_1 + \frac{17}{36}\eta_2^3\Big)b^L_{19} \\
& + \Big(3\eta_2^2 - \frac{2}{3}\eta_2^3 - \frac{7}{8}\eta_1 + \frac{5}{8}\eta_1^2 + 3\eta_2\eta_1 + \eta_2\eta_1^2 - \frac{3}{2}\eta_2 + \frac{17}{36}\eta_1^3\Big)b^L_{22} \\
& + \frac{\eta_3}{8}(21\eta_1^2 + 24\eta_1\eta_2 + 7\eta_2^2 - 15\eta_1 - 9\eta_2)b^L_{25} + \frac{\eta_3}{8}(21\eta_2^2 + 24\eta_2\eta_1 + 7\eta_1^2 - 15\eta_2 - 9\eta_1)b^L_{28} \\
& + \frac{7}{8}\eta_3(2\eta_1^2 + 6\eta_1\eta_2 + 2\eta_2^2 + 3\eta_1 + 3\eta_2)b^L_{31} + \frac{9}{8}\eta_3^2(3\eta_1+\eta_2)\tilde{b}^L_{34} + \frac{9}{8}\eta_3^2(3\eta_2+\eta_1)\tilde{b}^L_{37} + \eta_3^3\tilde{b}^L_{46}.
\end{aligned}
\tag{37}
$$

Proof. Assume s^L and s^R join C^2 across the common edge $\boldsymbol{p}_1\boldsymbol{p}_2$. To prove C^3 smoothness across the same edge, it suffices to prove that along $\boldsymbol{p}_1\boldsymbol{p}_2$ the functions $D^3_{\boldsymbol{p}_1\boldsymbol{p}_3}s^L$ and $D^3_{\boldsymbol{p}_1\boldsymbol{p}_3}s^R$ agree. Along the edge $\boldsymbol{p}_1\boldsymbol{p}_2$, the above functions are univariate C^0 linear splines with (interior) knots at the points $\boldsymbol{q}_{3,1}$, $\boldsymbol{q}_3$, and $\boldsymbol{q}_{3,2}$. Therefore, each of them is uniquely determined by its value at the two endpoints of the edge and by its value at the points $\boldsymbol{q}_{3,1}$, $\boldsymbol{q}_3$, and $\boldsymbol{q}_{3,2}$. From (28) we know that

$$
D^3_{\boldsymbol{p}_1\boldsymbol{p}_3} = \Big(\frac{1}{\eta_3}D_{\boldsymbol{p}_1\boldsymbol{p}_4} - \frac{\eta_2}{\eta_3}D_{\boldsymbol{p}_1\boldsymbol{p}_2}\Big)^3.
$$

By using the values in Tables 6–8 in the appendix together with those in Table 2, a direct computation provides the expressions of

$$
D^3_{\boldsymbol{p}_1\boldsymbol{p}_3}s^L(\boldsymbol{p}), \quad D^3_{\boldsymbol{p}_1\boldsymbol{p}_3}s^R(\boldsymbol{p}), \quad \boldsymbol{p}\in\{\boldsymbol{p}_1,\boldsymbol{q}_{3,1},\boldsymbol{q}_3,\boldsymbol{q}_{3,2},\boldsymbol{p}_2\}.
$$

By equating these expressions and taking into account the C^2 smoothness conditions, we obtain the conditions (33)–(37). □

Remark 10. Using the conversion between the bases (5) and (32), see Table 2, we can immediately rewrite the C^3 smoothness conditions provided in Theorem 9 solely in terms of coefficients of the basis (5).

Remark 11. A global basis for the space $\mathbb{S}^3_4(\mathcal{T}_{\mathrm{WS}_4})$ can be constructed by using the technique of minimal determining sets [13], following the same line of arguments as in [15, Section 4.2]. Even though both the local bases (5) and (32) may be used to this aim, the second one is preferable. Indeed, when using the basis (32), the locality of the smoothness conditions provided in Theorems 5 and 9 implies the local support of the global basis functions.

5. Conclusion

We have addressed the 51 dimensional space of C^3 quartic splines on the WS_4 split of a given triangle. For this space we have constructed a (scaled) simplex spline basis and we have provided a unisolvent Hermite interpolation problem which allows us to locally characterize any function belonging to the space of C^3 quartic splines on the WS_4 refinement of a given triangulation. These results are a quartic extension of those obtained in [5] and [15] for the PS-12 split and the WS_3 split, respectively, i.e., for the quadratic and the cubic members of the Wang–Shi split family.

As in the quadratic and cubic cases, the basis is a B-spline basis within a single macro-triangle but globally it behaves like a Bernstein basis across macro-triangles. We have proved that the basis has many desirable B-spline properties including that it forms a nonnegative partition of unity and enjoys a Marsden-like identity. The restriction of each basis function onto a boundary edge of the macro-triangle reduces to a classical univariate C^3 quartic B-spline.

The basis can be equipped with control points and a control net. The control net is unusual in the sense that it incorporates three pairs of coincident domain points. A proper 48 dimensional subspace containing quartic polynomials has been identified for which a classical control net (based on different domain points) with triangular and hexagonal connectivity can be naturally constructed. Furthermore, explicit conditions for smoothness up to the third order across a common edge of two macro-triangles have been derived in terms of the respective control points. We have also proposed an alternative basis for the space $\mathbb{S}^3_4(\Delta_{\mathrm{WS}_4})$ that simplifies the imposition of C^3 smoothness conditions across edges.

The technique of minimal determining sets can be used to build (stable) locally supported global basis functions for the space $\mathbb{S}^3_4(\mathcal{T}_{\mathrm{WS}_4})$; see Remark 11. In addition, the availability of such a global basis allows us to show the optimal approximation power of the space using a similar line of arguments as in [15, Section 4.2].

For computation with splines belonging to $\mathbb{S}^3_4(\mathcal{T}_{\mathrm{WS}_4})$, it is convenient to work directly with the local representations provided by the simplex spline basis (5) or the alternative basis (32). The evaluation of the simplex spline basis functions can be achieved by applying the recurrence relation (B-recurrence) of simplex splines; see Section 2.2. However, it might be more convenient to use a lookup-table approach as proposed in [15, Section 5.1] for the C^2 cubic case. The explicit expressions of the simplex spline basis elements can be stored in a suitable table and then accessed by a search algorithm based on boolean vectors. The alternative basis functions in (32) can be immediately deduced from the previous ones by means of the conversion matrix in Table 2.

The local simplex spline basis makes the treatment of the complex geometry of the WS_4 split more affordable because it intrinsically avoids to consider separate polynomial representations on each of the 250 polygonal subelements of the split. This transparency of the WS_4 split to the user offers a pathway for effective use of the interesting space of C^3 quartic splines on the WS_4 refinement of a given triangulation.

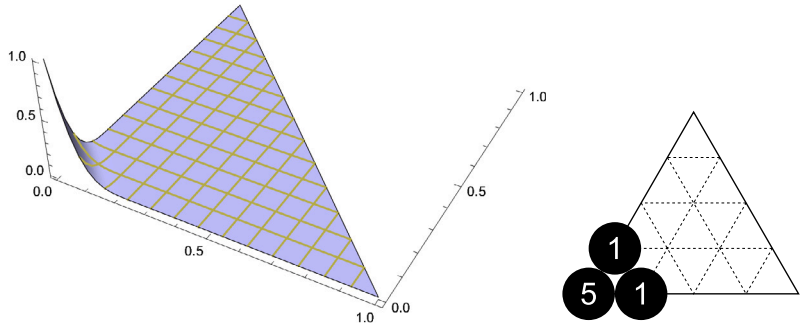

Fig. 11. The simplex spline basis function B_1 and its support.

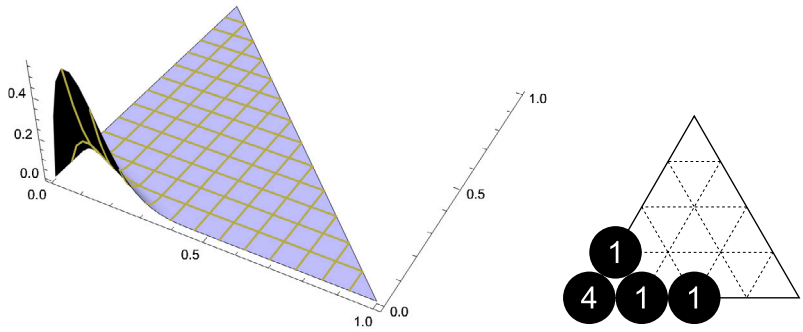

Fig. 12. The simplex spline basis function B_4 and its support.

Generalizations of the presented construction to higher degrees $d \geq 5$ would be desirable. Extensions to splines in three or more variables would be of great interest as well. However, neither appears straightforward.

Data availability

No data was used for the research described in the article.

Acknowledgements

This work was supported by the MUR Excellence Department Project MatMod@TOV (CUP E83C23000330006) awarded to the Department of Mathematics of the University of Rome Tor Vergata and by the National Research Center in High Performance Computing, Big Data and Quantum Computing (CUP E83C22003230001). The authors are grateful to CIRM, Luminy for the Research in Residence support (2809). C. Manni and H. Speleers are members of Gruppo Nazionale per il Calcolo Scientifico, Istituto Nazionale di Alta Matematica.

Appendix A

In this appendix, we collect data related to the simplex spline basis functions $B_1, \ldots, B_{51}$ in (5) that were used in the proofs and might be useful for practical purposes as well. The different types of basis functions are depicted in Figs. 11–21. The values of the operators ρ_i in (7)–(9) applied to the B_j's are collected in Tables 3–5. The values of the operators ς_i in (25)–(27) applied to the B_j's are collected in Tables 6–8.

References

[1] P. Alfeld, L.L. Schumaker, Smooth macro-elements based on Powell–Sabin triangle splits, Adv. Comput. Math. 16 (2002) 29–46.
[2] C.K. Chui, R.-H. Wang, Multivariate spline spaces, J. Math. Anal. Appl. 94 (1983) 197–221.
[3] P.G. Ciarlet, The Finite Element Method for Elliptic Problems, Classics in Applied Mathematics, vol. 40, SIAM, Philadelphia, 2002.
[4] R.W. Clough, J.L. Tocher, Finite element stiffness matrices for analysis of plates in bending, in: Proceedings of the Conference on Matrix Methods in Structural Mechanics, Wright-Patterson Air Force Base, 1965, pp. 515–545.
[5] E. Cohen, T. Lyche, R.F. Riesenfeld, A B-spline-like basis for the Powell–Sabin 12-split based on simplex splines, Math. Comput. 82 (2013) 1667–1707.
[6] J.A. Cottrell, T.J.R. Hughes, Y. Bazilevs, Isogeometric Analysis: Toward Integration of CAD and FEA, Wiley Publishing, 2009.
[7] P. Dierckx, On calculating normalized Powell–Sabin B-splines, Comput. Aided Geom. Des. 15 (1997) 61–78.
[8] J. Grošelj, A normalized representation of super splines of arbitrary degree on Powell–Sabin triangulations, BIT Numer. Math. 56 (2016) 1257–1280.
[9] J. Grošelj, M. Knez, Generalized Clough–Tocher splines for CAGD and FEM, Comput. Methods Appl. Mech. Eng. 395 (2022) 114983.

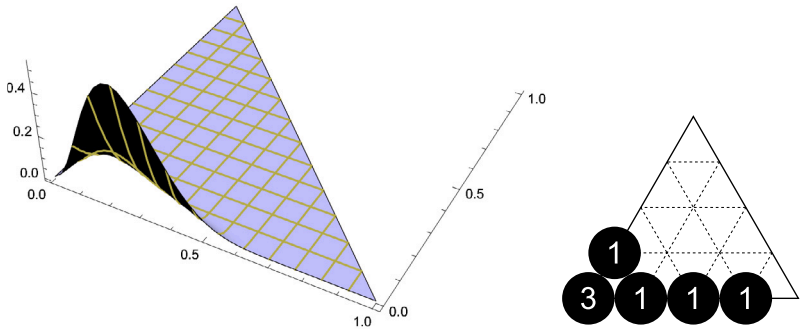

Fig. 13. The simplex spline basis function B_{10} and its support.

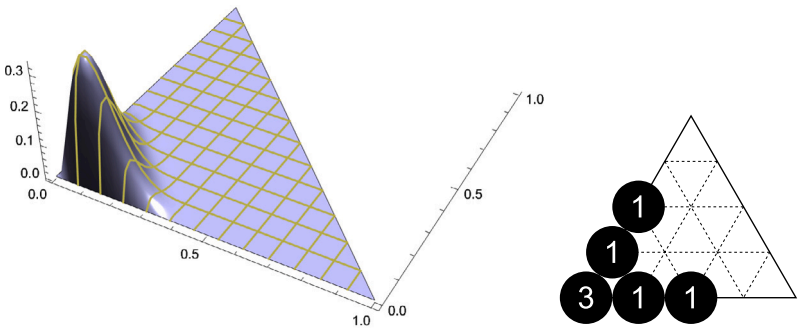

Fig. 14. The simplex spline basis function B_{16} and its support.

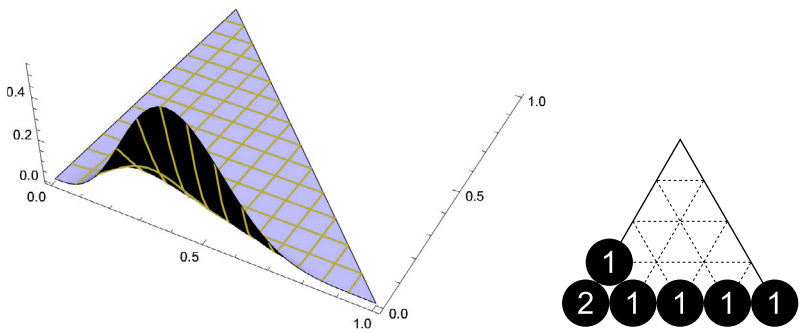

Fig. 15. The simplex spline basis function B_{19} and its support.

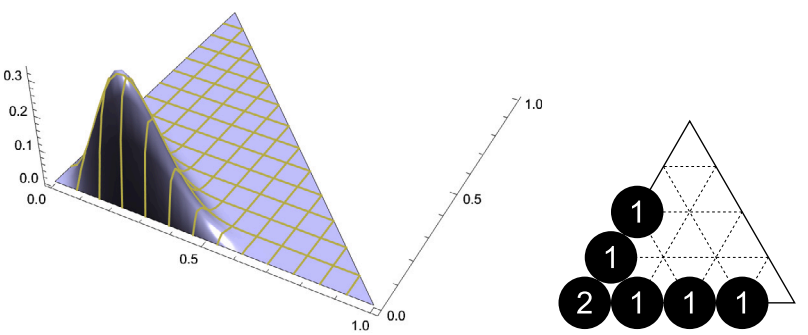

Fig. 16. The simplex spline basis function B_{25} and its support.

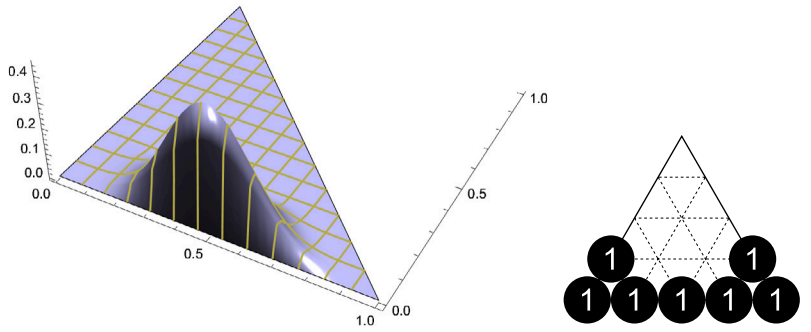

Fig. 17. The simplex spline basis function B_{31} and its support.

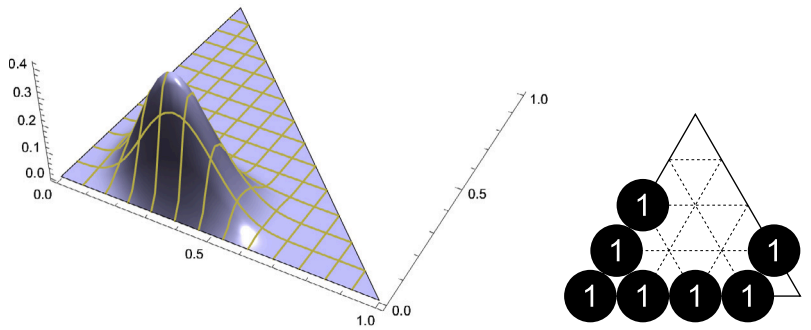

Fig. 18. The simplex spline basis function B_{34} and its support.

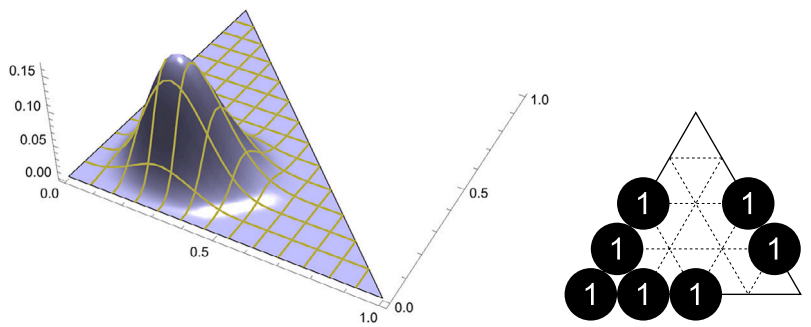

Fig. 19. The simplex spline basis function B_{40} and its support.

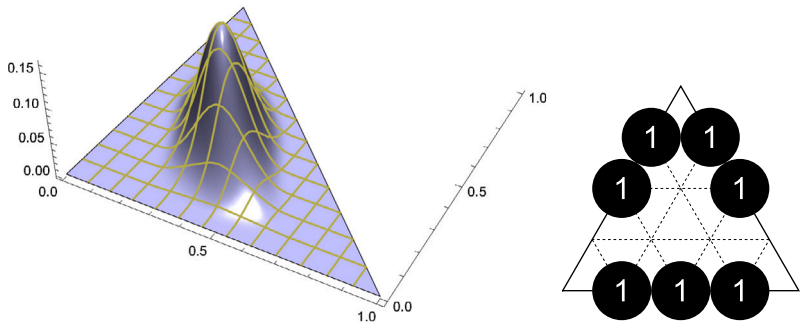

Fig. 20. The simplex spline basis function B_{46} and its support.

Table 3
Values of $\rho_i(B_j)$ for $i = 1,\dots,51$, $j = 1,\dots,18$, where ρ_i is defined in (7), (8), and (9).

	B_1	B_2	B_3	B_4	B_5	B_6	B_7	B_8	B_9	B_{10}	B_{11}	B_{12}	B_{13}	B_{14}	B_{15}	B_{16}	B_{17}	B_{18}
ρ_1	1	0	0	0	0	0	0	0	0	0	0	0	0	0	0	0	0	0
ρ_2	0	1	0	0	0	0	0	0	0	0	0	0	0	0	0	0	0	0
ρ_3	0	0	1	0	0	0	0	0	0	0	0	0	0	0	0	0	0	0
ρ_4	−16	0	0	16	0	0	0	0	0	0	0	0	0	0	0	0	0	0
ρ_5	−16	0	0	0	16	0	0	0	0	0	0	0	0	0	0	0	0	0
ρ_6	0	−16	0	0	0	16	0	0	0	0	0	0	0	0	0	0	0	0
ρ_7	0	−16	0	0	0	0	16	0	0	0	0	0	0	0	0	0	0	0
ρ_8	0	0	−16	0	0	0	0	16	0	0	0	0	0	0	0	0	0	0
ρ_9	0	0	−16	0	0	0	0	0	16	0	0	0	0	0	0	0	0	0
ρ_{10}	192	0	0	−288	0	0	0	0	0	96	0	0	0	0	0	0	0	0
ρ_{11}	192	0	0	0	−288	0	0	0	0	0	96	0	0	0	0	0	0	0
ρ_{12}	0	192	0	0	0	−288	0	0	0	0	0	96	0	0	0	0	0	0
ρ_{13}	0	192	0	0	0	0	−288	0	0	0	0	0	96	0	0	0	0	0
ρ_{14}	0	0	192	0	0	0	0	−288	0	0	0	0	0	96	0	0	0	0
ρ_{15}	0	0	192	0	0	0	0	0	−288	0	0	0	0	0	96	0	0	0
ρ_{16}	192	0	0	−192	−192	0	0	0	0	0	0	0	0	0	0	192	0	0
ρ_{17}	0	192	0	0	0	−192	−192	0	0	0	0	0	0	0	0	0	192	0
ρ_{18}	0	0	192	0	0	0	0	−192	−192	0	0	0	0	0	0	0	0	192
ρ_{19}	−1536	0	0	2688	0	0	0	0	0	−1408	0	0	0	0	0	0	0	0
ρ_{20}	−1536	0	0	0	2688	0	0	0	0	0	−1408	0	0	0	0	0	0	0
ρ_{21}	0	−1536	0	0	0	2688	0	0	0	0	0	−1408	0	0	0	0	0	0
ρ_{22}	0	−1536	0	0	0	0	2688	0	0	0	0	0	−1408	0	0	0	0	0
ρ_{23}	0	0	−1536	0	0	0	0	2688	0	0	0	0	0	−1408	0	0	0	0
ρ_{24}	0	0	−1536	0	0	0	0	0	2688	0	0	0	0	0	−1408	0	0	0
ρ_{25}	−1536	0	0	2304	1536	0	0	0	0	−768	0	0	0	0	0	−2304	0	0
ρ_{26}	−1536	0	0	1536	2304	0	0	0	0	0	−768	0	0	0	0	−2304	0	0
ρ_{27}	0	−1536	0	0	0	2304	1536	0	0	0	0	−768	0	0	0	0	−2304	0
ρ_{28}	0	−1536	0	0	0	1536	2304	0	0	0	0	0	−768	0	0	0	−2304	0
ρ_{29}	0	0	−1536	0	0	0	0	2304	1536	0	0	0	0	−768	0	0	0	−2304
ρ_{30}	0	0	−1536	0	0	0	0	1536	2304	0	0	0	0	0	−768	0	0	−2304
ρ_{31}	0	0	0	0	0	0	0	0	0	$-\frac{20}{9}$	0	0	$-\frac{20}{9}$	0	0	0	0	0
ρ_{32}	0	0	0	0	0	0	0	0	0	0	0	$-\frac{20}{9}$	0	0	$-\frac{20}{9}$	0	0	0
ρ_{33}	0	0	0	0	0	0	0	0	0	0	$-\frac{20}{9}$	0	0	$-\frac{20}{9}$	0	0	0	0
ρ_{34}	0	0	0	$\frac{147}{2}$	0	0	0	0	0	$\frac{613}{6}$	0	0	0	0	0	−120	0	0
ρ_{35}	0	0	0	0	$\frac{147}{2}$	0	0	0	0	0	$\frac{613}{6}$	0	0	0	0	−120	0	0
ρ_{36}	0	0	0	0	0	$\frac{147}{2}$	0	0	0	0	0	$\frac{613}{6}$	0	0	0	0	−120	0
ρ_{37}	0	0	0	0	0	0	$\frac{147}{2}$	0	0	0	0	0	$\frac{613}{6}$	0	0	0	−120	0
ρ_{38}	0	0	0	0	0	0	0	$\frac{147}{2}$	0	0	0	0	0	$\frac{613}{6}$	0	0	0	−120
ρ_{39}	0	0	0	0	0	0	0	0	$\frac{147}{2}$	0	0	0	0	0	$\frac{613}{6}$	0	0	−120
ρ_{40}	0	0	0	−1029	0	0	0	0	0	$-\frac{1387}{3}$	0	0	0	0	0	1896	0	0
ρ_{41}	0	0	0	0	−1029	0	0	0	0	0	$-\frac{1387}{3}$	0	0	0	0	1896	0	0
ρ_{42}	0	0	0	0	0	−1029	0	0	0	0	0	$-\frac{1387}{3}$	0	0	0	0	1896	0
ρ_{43}	0	0	0	0	0	0	−1029	0	0	0	0	0	$-\frac{1387}{3}$	0	0	0	1896	0
ρ_{44}	0	0	0	0	0	0	0	−1029	0	0	0	0	0	$-\frac{1387}{3}$	0	0	0	1896
ρ_{45}	0	0	0	0	0	0	0	0	−1029	0	0	0	0	0	$-\frac{1387}{3}$	0	0	1896
ρ_{46}	0	0	0	0	0	0	0	0	0	$-\frac{4000}{3}$	0	0	$-\frac{4000}{3}$	0	0	0	0	0
ρ_{47}	0	0	0	0	0	0	0	0	0	0	0	$-\frac{4000}{3}$	0	0	$-\frac{4000}{3}$	0	0	0
ρ_{48}	0	0	0	0	0	0	0	0	0	0	$-\frac{4000}{3}$	0	0	$-\frac{4000}{3}$	0	0	0	0
ρ_{49}	0	0	0	0	0	0	0	0	0	0	0	0	0	0	0	0	0	0
ρ_{50}	0	0	0	0	0	0	0	0	0	0	0	0	0	0	0	0	0	0
ρ_{51}	0	0	0	0	0	0	0	0	0	0	0	0	0	0	0	0	0	0

Table 4
Values of $\rho_i(B_j)$ for $i = 1,\dots,51$, $j = 19,\dots,39$, where ρ_i is defined in (7), (8), and (9).

	B_{19}	B_{20}	B_{21}	B_{22}	B_{23}	B_{24}	B_{25}	B_{26}	B_{27}	B_{28}	B_{29}	B_{30}	B_{31}	B_{32}	B_{33}	B_{34}	B_{35}	B_{36}	B_{37}	B_{38}	B_{39}
ρ_1	0	0	0	0	0	0	0	0	0	0	0	0	0	0	0	0	0	0	0	0	0
ρ_2	0	0	0	0	0	0	0	0	0	0	0	0	0	0	0	0	0	0	0	0	0
ρ_3	0	0	0	0	0	0	0	0	0	0	0	0	0	0	0	0	0	0	0	0	0
ρ_4	0	0	0	0	0	0	0	0	0	0	0	0	0	0	0	0	0	0	0	0	0
ρ_5	0	0	0	0	0	0	0	0	0	0	0	0	0	0	0	0	0	0	0	0	0
ρ_6	0	0	0	0	0	0	0	0	0	0	0	0	0	0	0	0	0	0	0	0	0
ρ_7	0	0	0	0	0	0	0	0	0	0	0	0	0	0	0	0	0	0	0	0	0
ρ_8	0	0	0	0	0	0	0	0	0	0	0	0	0	0	0	0	0	0	0	0	0
ρ_9	0	0	0	0	0	0	0	0	0	0	0	0	0	0	0	0	0	0	0	0	0
ρ_{10}	0	0	0	0	0	0	0	0	0	0	0	0	0	0	0	0	0	0	0	0	0
ρ_{11}	0	0	0	0	0	0	0	0	0	0	0	0	0	0	0	0	0	0	0	0	0
ρ_{12}	0	0	0	0	0	0	0	0	0	0	0	0	0	0	0	0	0	0	0	0	0
ρ_{13}	0	0	0	0	0	0	0	0	0	0	0	0	0	0	0	0	0	0	0	0	0
ρ_{14}	0	0	0	0	0	0	0	0	0	0	0	0	0	0	0	0	0	0	0	0	0
ρ_{15}	0	0	0	0	0	0	0	0	0	0	0	0	0	0	0	0	0	0	0	0	0
ρ_{16}	0	0	0	0	0	0	0	0	0	0	0	0	0	0	0	0	0	0	0	0	0
ρ_{17}	0	0	0	0	0	0	0	0	0	0	0	0	0	0	0	0	0	0	0	0	0
ρ_{18}	0	0	0	0	0	0	0	0	0	0	0	0	0	0	0	0	0	0	0	0	0
ρ_{19}	256	0	0	0	0	0	0	0	0	0	0	0	0	0	0	0	0	0	0	0	0
ρ_{20}	0	256	0	0	0	0	0	0	0	0	0	0	0	0	0	0	0	0	0	0	0
ρ_{21}	0	0	256	0	0	0	0	0	0	0	0	0	0	0	0	0	0	0	0	0	0
ρ_{22}	0	0	0	256	0	0	0	0	0	0	0	0	0	0	0	0	0	0	0	0	0
ρ_{23}	0	0	0	0	256	0	0	0	0	0	0	0	0	0	0	0	0	0	0	0	0
ρ_{24}	0	0	0	0	0	256	0	0	0	0	0	0	0	0	0	0	0	0	0	0	0
ρ_{25}	0	0	0	0	0	0	768	0	0	0	0	0	0	0	0	0	0	0	0	0	0
ρ_{26}	0	0	0	0	0	0	0	768	0	0	0	0	0	0	0	0	0	0	0	0	0
ρ_{27}	0	0	0	0	0	0	0	0	768	0	0	0	0	0	0	0	0	0	0	0	0
ρ_{28}	0	0	0	0	0	0	0	0	0	768	0	0	0	0	0	0	0	0	0	0	0
ρ_{29}	0	0	0	0	0	0	0	0	0	0	768	0	0	0	0	0	0	0	0	0	0
ρ_{30}	0	0	0	0	0	0	0	0	0	0	0	768	0	0	0	0	0	0	0	0	0
ρ_{31}	$-\frac{88}{9}$	0	0	$-\frac{88}{9}$	0	0	$\frac{8}{3}$	0	0	$\frac{8}{3}$	0	0	$\frac{56}{3}$	0	0	0	0	0	0	0	0
ρ_{32}	0	0	$-\frac{88}{9}$	0	0	$-\frac{88}{9}$	0	0	$\frac{8}{3}$	0	0	$\frac{8}{3}$	0	$\frac{56}{3}$	0	0	0	0	0	0	0
ρ_{33}	0	$-\frac{88}{9}$	0	0	$-\frac{88}{9}$	0	0	$\frac{8}{3}$	0	0	$\frac{8}{3}$	0	0	0	$\frac{56}{3}$	0	0	0	0	0	0
ρ_{34}	$\frac{95}{6}$	0	0	$\frac{169}{2}$	0	0	−152	48	0	0	0	0	−196	0	0	144	0	0	0	0	0
ρ_{35}	0	$\frac{95}{6}$	0	0	$\frac{169}{2}$	0	48	−152	0	0	0	0	0	0	−196	0	144	0	0	0	0
ρ_{36}	0	0	$\frac{95}{6}$	0	0	$\frac{169}{2}$	0	0	−152	48	0	0	0	−196	0	0	0	144	0	0	0
ρ_{37}	$\frac{169}{2}$	0	0	$\frac{95}{6}$	0	0	0	0	48	−152	0	0	−196	0	0	0	0	0	144	0	0
ρ_{38}	0	$\frac{169}{2}$	0	0	$\frac{95}{6}$	0	0	0	0	0	−152	48	0	0	−196	0	0	0	0	144	0
ρ_{39}	0	0	$\frac{169}{2}$	0	0	$\frac{95}{6}$	0	0	0	0	48	−152	0	−196	0	0	0	0	0	0	144
ρ_{40}	$-\frac{131}{3}$	0	0	−2197	0	0	744	−1120	0	0	0	0	5124	0	0	−4320	384	0	0	0	0
ρ_{41}	0	$-\frac{131}{3}$	0	0	−2197	0	−1120	744	0	0	0	0	0	0	5124	384	−4320	0	0	0	0
ρ_{42}	0	0	$-\frac{131}{3}$	0	0	−2197	0	0	744	−1120	0	0	0	5124	0	0	0	−4320	384	0	0
ρ_{43}	−2197	0	0	$-\frac{131}{3}$	0	0	0	0	−1120	744	0	0	5124	0	0	0	0	384	−4320	0	0
ρ_{44}	0	−2197	0	0	$-\frac{131}{3}$	0	0	0	0	0	744	−1120	0	0	5124	0	0	0	0	−4320	384
ρ_{45}	0	0	−2197	0	0	$-\frac{131}{3}$	0	0	0	0	−1120	744	0	5124	0	0	0	0	0	384	−4320
ρ_{46}	$-\frac{464}{3}$	0	0	$-\frac{464}{3}$	0	0	2496	0	0	2496	0	0	3360	0	0	−3456	0	0	−3456	0	0
ρ_{47}	0	0	$-\frac{464}{3}$	0	0	$-\frac{464}{3}$	0	0	2496	0	0	2496	0	3360	0	0	0	−3456	0	0	−3456
ρ_{48}	0	$-\frac{464}{3}$	0	0	$-\frac{464}{3}$	0	0	2496	0	0	2496	0	0	0	3360	0	−3456	0	0	−3456	0
ρ_{49}	0	0	0	0	0	0	0	0	0	0	0	0	0	0	0	$\frac{27}{640}$	$\frac{1}{1920}$	$\frac{1}{1920}$	$\frac{27}{640}$	0	0
ρ_{50}	0	0	0	0	0	0	0	0	0	0	0	0	0	0	0	0	0	$\frac{27}{640}$	$\frac{1}{1920}$	$\frac{1}{1920}$	$\frac{27}{640}$
ρ_{51}	0	0	0	0	0	0	0	0	0	0	0	0	0	0	0	$\frac{1}{1920}$	$\frac{27}{640}$	0	0	$\frac{27}{640}$	$\frac{1}{1920}$

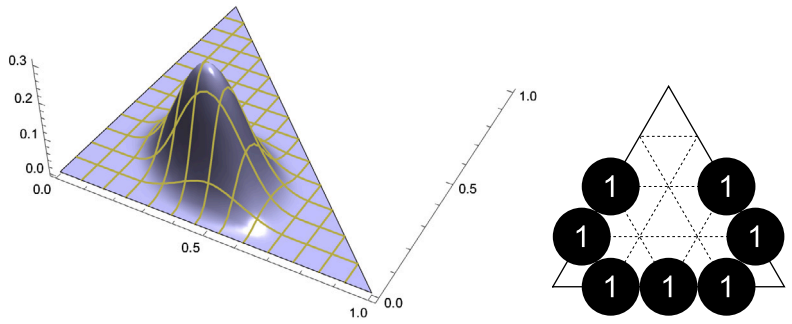

Fig. 21. The simplex spline basis function B_{49} and its support.

Table 5
Values of $\rho_i(B_j)$ for $i = 1,\dots,51$, $j = 40,\dots,51$, where ρ_i is defined in (7), (8), and (9).

	B_{40}	B_{41}	B_{42}	B_{43}	B_{44}	B_{45}	B_{46}	B_{47}	B_{48}	B_{49}	B_{50}	B_{51}
ρ_1	0	0	0	0	0	0	0	0	0	0	0	0
ρ_2	0	0	0	0	0	0	0	0	0	0	0	0
ρ_3	0	0	0	0	0	0	0	0	0	0	0	0
ρ_4	0	0	0	0	0	0	0	0	0	0	0	0
ρ_5	0	0	0	0	0	0	0	0	0	0	0	0
ρ_6	0	0	0	0	0	0	0	0	0	0	0	0
ρ_7	0	0	0	0	0	0	0	0	0	0	0	0
ρ_8	0	0	0	0	0	0	0	0	0	0	0	0
ρ_9	0	0	0	0	0	0	0	0	0	0	0	0
ρ_{10}	0	0	0	0	0	0	0	0	0	0	0	0
ρ_{11}	0	0	0	0	0	0	0	0	0	0	0	0
ρ_{12}	0	0	0	0	0	0	0	0	0	0	0	0
ρ_{13}	0	0	0	0	0	0	0	0	0	0	0	0
ρ_{14}	0	0	0	0	0	0	0	0	0	0	0	0
ρ_{15}	0	0	0	0	0	0	0	0	0	0	0	0
ρ_{16}	0	0	0	0	0	0	0	0	0	0	0	0
ρ_{17}	0	0	0	0	0	0	0	0	0	0	0	0
ρ_{18}	0	0	0	0	0	0	0	0	0	0	0	0
ρ_{19}	0	0	0	0	0	0	0	0	0	0	0	0
ρ_{20}	0	0	0	0	0	0	0	0	0	0	0	0
ρ_{21}	0	0	0	0	0	0	0	0	0	0	0	0
ρ_{22}	0	0	0	0	0	0	0	0	0	0	0	0
ρ_{23}	0	0	0	0	0	0	0	0	0	0	0	0
ρ_{24}	0	0	0	0	0	0	0	0	0	0	0	0
ρ_{25}	0	0	0	0	0	0	0	0	0	0	0	0
ρ_{26}	0	0	0	0	0	0	0	0	0	0	0	0
ρ_{27}	0	0	0	0	0	0	0	0	0	0	0	0
ρ_{28}	0	0	0	0	0	0	0	0	0	0	0	0
ρ_{29}	0	0	0	0	0	0	0	0	0	0	0	0
ρ_{30}	0	0	0	0	0	0	0	0	0	0	0	0
ρ_{31}	0	0	0	0	0	0	0	0	0	0	0	0
ρ_{32}	0	0	0	0	0	0	0	0	0	0	0	0
ρ_{33}	0	0	0	0	0	0	0	0	0	0	0	0
ρ_{34}	0	0	0	0	0	0	0	0	0	0	0	0
ρ_{35}	0	0	0	0	0	0	0	0	0	0	0	0
ρ_{36}	0	0	0	0	0	0	0	0	0	0	0	0
ρ_{37}	0	0	0	0	0	0	0	0	0	0	0	0
ρ_{38}	0	0	0	0	0	0	0	0	0	0	0	0
ρ_{39}	0	0	0	0	0	0	0	0	0	0	0	0
ρ_{40}	768	256	0	0	0	0	0	0	0	0	0	0
ρ_{41}	256	768	0	0	0	0	0	0	0	0	0	0
ρ_{42}	0	0	768	256	0	0	0	0	0	0	0	0
ρ_{43}	0	0	256	768	0	0	0	0	0	0	0	0
ρ_{44}	0	0	0	0	768	256	0	0	0	0	0	0
ρ_{45}	0	0	0	0	256	768	0	0	0	0	0	0
ρ_{46}	0	0	0	0	0	0	96	0	0	1440	0	0
ρ_{47}	0	0	0	0	0	0	0	96	0	0	1440	0
ρ_{48}	0	0	0	0	0	0	0	0	96	0	0	1440
ρ_{49}	$\frac{31}{320}$	$\frac{11}{720}$	$\frac{11}{720}$	$\frac{31}{320}$	$\frac{1}{72}$	$\frac{1}{72}$	$\frac{43}{384}$	$\frac{303}{2560}$	$\frac{303}{2560}$	$\frac{33}{128}$	$\frac{43}{1536}$	$\frac{43}{1536}$
ρ_{50}	$\frac{1}{72}$	$\frac{1}{72}$	$\frac{31}{320}$	$\frac{11}{720}$	$\frac{11}{720}$	$\frac{31}{320}$	$\frac{303}{2560}$	$\frac{43}{384}$	$\frac{303}{2560}$	$\frac{43}{1536}$	$\frac{33}{128}$	$\frac{43}{1536}$
ρ_{51}	$\frac{11}{720}$	$\frac{31}{320}$	$\frac{1}{72}$	$\frac{1}{72}$	$\frac{31}{320}$	$\frac{11}{720}$	$\frac{303}{2560}$	$\frac{303}{2560}$	$\frac{43}{384}$	$\frac{43}{1536}$	$\frac{43}{1536}$	$\frac{33}{128}$

Table 6
Values of $\varsigma_i(B_j)$ for $i = 1, \dots, 38$, $j = 1, \dots, 18$, where ς_i is defined in (25), (26), and (27).

	B_1	B_2	B_3	B_4	B_5	B_6	B_7	B_8	B_9	B_{10}	B_{11}	B_{12}	B_{13}	B_{14}	B_{15}	B_{16}	B_{17}	B_{18}
ς_1	−16	0	0	0	16	0	0	0	0	0	0	0	0	0	0	0	0	0
ς_2	−16	0	0	16	0	0	0	0	0	0	0	0	0	0	0	0	0	0
ς_3	0	0	0	0	0	0	0	0	0	$-\frac{8}{9}$	0	0	$-\frac{16}{9}$	0	0	0	0	0
ς_4	0	0	0	0	0	0	0	0	0	$-\frac{8}{9}$	0	0	$\frac{8}{9}$	0	0	0	0	0
ς_5	0	0	0	0	0	16	−16	0	0	0	0	0	0	0	0	0	0	0
ς_6	0	16	0	0	0	0	−16	0	0	0	0	0	0	0	0	0	0	0
ς_7	192	0	0	0	−288	0	0	0	0	0	96	0	0	0	0	0	0	0
ς_8	192	0	0	−192	−192	0	0	0	0	0	0	0	0	0	0	192	0	0
ς_9	192	0	0	−288	0	0	0	0	0	96	0	0	0	0	0	0	0	0
ς_{10}	0	0	0	96	0	0	0	0	0	96	0	0	0	0	0	−144	0	0
ς_{11}	0	0	0	48	0	0	0	0	0	−16	0	0	0	0	0	−48	0	0
ς_{12}	0	0	0	24	0	0	0	0	0	$-\frac{88}{3}$	0	0	0	0	0	0	0	0
ς_{13}	0	0	0	0	0	0	24	0	0	0	0	0	$\frac{296}{3}$	0	0	0	−48	0
ς_{14}	0	0	0	0	0	0	−24	0	0	0	0	0	$-\frac{40}{3}$	0	0	0	48	0
ς_{15}	0	0	0	0	0	0	24	0	0	0	0	0	$-\frac{88}{3}$	0	0	0	0	0
ς_{16}	0	0	0	0	0	96	96	0	0	0	0	96	96	0	0	0	−384	0
ς_{17}	0	0	0	0	0	192	−96	0	0	0	0	0	96	0	0	0	−192	0
ς_{18}	0	192	0	0	0	0	−288	0	0	0	0	0	96	0	0	0	0	0
ς_{19}	−1536	0	0	0	2688	0	0	0	0	0	−1408	0	0	0	0	0	0	0
ς_{20}	−1536	0	0	1536	2304	0	0	0	0	0	−768	0	0	0	0	−2304	0	0
ς_{21}	−1536	0	0	2304	1536	0	0	0	0	−768	0	0	0	0	0	−2304	0	0
ς_{22}	−1536	0	0	2688	0	0	0	0	0	−1408	0	0	0	0	0	0	0	0
ς_{23}	0	0	0	−1536	0	0	0	0	0	0	0	0	0	0	0	2688	0	0
ς_{24}	0	0	0	−768	0	0	0	0	0	768	0	0	0	0	0	1152	0	0
ς_{25}	0	0	0	−384	0	0	0	0	0	640	0	0	0	0	0	384	0	0
ς_{26}	0	0	0	−192	0	0	0	0	0	$\frac{1216}{3}$	0	0	0	0	0	0	0	0
ς_{27}	0	0	0	0	0	0	0	0	0	−2304	0	0	$-\frac{2048}{3}$	0	0	0	0	0
ς_{28}	0	0	0	0	0	0	0	0	0	−768	0	0	$\frac{1024}{3}$	0	0	0	0	0
ς_{29}	0	0	0	0	0	0	0	0	0	−256	0	0	$-\frac{512}{3}$	0	0	0	0	0
ς_{30}	0	0	0	0	0	0	0	0	0	$-\frac{256}{3}$	0	0	$\frac{256}{3}$	0	0	0	0	0
ς_{31}	0	0	0	0	0	0	−192	0	0	0	0	0	$-\frac{2368}{3}$	0	0	0	384	0
ς_{32}	0	0	0	0	0	0	192	0	0	0	0	0	$\frac{320}{3}$	0	0	0	−384	0
ς_{33}	0	0	0	0	0	0	−192	0	0	0	0	0	$\frac{704}{3}$	0	0	0	384	0
ς_{34}	0	0	0	0	0	0	192	0	0	0	0	0	$-\frac{1216}{3}$	0	0	0	0	0
ς_{35}	0	0	0	0	0	384	−384	0	0	0	0	896	−896	0	0	0	0	0
ς_{36}	0	0	0	0	0	768	384	0	0	0	0	768	−128	0	0	0	−2304	0
ς_{37}	0	0	0	0	0	1536	−384	0	0	0	0	0	640	0	0	0	−2304	0
ς_{38}	0	1536	0	0	0	0	−2688	0	0	0	0	0	1408	0	0	0	0	0

Table 7
Values of $\varsigma_i(B_j)$ for $i = 1, \dots, 38$, $j = 19, \dots, 39$, where ς_i is defined in (25), (26), and (27).

	B_{19}	B_{20}	B_{21}	B_{22}	B_{23}	B_{24}	B_{25}	B_{26}	B_{27}	B_{28}	B_{29}	B_{30}	B_{31}	B_{32}	B_{33}	B_{34}	B_{35}	B_{36}	B_{37}	B_{38}	B_{39}
ς_1	0	0	0	0	0	0	0	0	0	0	0	0	0	0	0	0	0	0	0	0	0
ς_2	0	0	0	0	0	0	0	0	0	0	0	0	0	0	0	0	0	0	0	0	0
ς_3	$-\frac{32}{3}$	0	0	$-\frac{80}{9}$	0	0	$\frac{8}{3}$	0	0	$\frac{8}{3}$	0	0	$\frac{56}{3}$	0	0	0	0	0	0	0	0
ς_4	$-\frac{16}{9}$	0	0	$\frac{16}{9}$	0	0	0	0	0	0	0	0	0	0	0	0	0	0	0	0	0
ς_5	0	0	0	0	0	0	0	0	0	0	0	0	0	0	0	0	0	0	0	0	0
ς_6	0	0	0	0	0	0	0	0	0	0	0	0	0	0	0	0	0	0	0	0	0
ς_7	0	0	0	0	0	0	0	0	0	0	0	0	0	0	0	0	0	0	0	0	0
ς_8	0	0	0	0	0	0	0	0	0	0	0	0	0	0	0	0	0	0	0	0	0
ς_9	0	0	0	0	0	0	0	0	0	0	0	0	0	0	0	0	0	0	0	0	0
ς_{10}	0	0	0	72	0	0	−144	48	0	0	0	0	−168	0	0	144	0	0	0	0	0
ς_{11}	−32	0	0	−24	0	0	16	0	0	0	0	0	56	0	0	0	0	0	0	0	0
ς_{12}	$-\frac{8}{3}$	0	0	8	0	0	0	0	0	0	0	0	0	0	0	0	0	0	0	0	0
ς_{13}	128	0	0	$\frac{184}{3}$	0	0	0	0	48	−176	0	0	−280	0	0	0	0	0	144	0	0
ς_{14}	32	0	0	$\frac{88}{3}$	0	0	0	0	0	−16	0	0	−56	0	0	0	0	0	0	0	0
ς_{15}	8	0	0	$-\frac{8}{3}$	0	0	0	0	0	0	0	0	0	0	0	0	0	0	0	0	0
ς_{16}	0	0	0	0	0	0	0	0	0	0	0	0	0	0	0	0	0	0	0	0	0
ς_{17}	0	0	0	0	0	0	0	0	0	0	0	0	0	0	0	0	0	0	0	0	0
ς_{18}	0	0	0	0	0	0	0	0	0	0	0	0	0	0	0	0	0	0	0	0	0
ς_{19}	0	256	0	0	0	0	0	0	0	0	0	0	0	0	0	0	0	0	0	0	0
ς_{20}	0	0	0	0	0	0	0	768	0	0	0	0	0	0	0	0	0	0	0	0	0
ς_{21}	0	0	0	0	0	0	768	0	0	0	0	0	0	0	0	0	0	0	0	0	0
ς_{22}	256	0	0	0	0	0	0	0	0	0	0	0	0	0	0	0	0	0	0	0	0
ς_{23}	0	0	0	−1728	0	0	0	−1408	0	0	0	0	4032	0	0	−3456	384	0	0	0	0
ς_{24}	0	0	0	576	0	0	−1152	−384	0	0	0	0	−1344	0	0	1152	0	0	0	0	0
ς_{25}	−256	0	0	−192	0	0	−640	0	0	0	0	0	448	0	0	0	0	0	0	0	0
ς_{26}	$-\frac{832}{3}$	0	0	64	0	0	0	0	0	0	0	0	0	0	0	0	0	0	0	0	0
ς_{27}	1024	0	0	$-\frac{2176}{3}$	0	0	4032	0	0	1344	0	0	2688	0	0	−5184	0	0	−1728	0	0
ς_{28}	1024	0	0	$-\frac{640}{3}$	0	0	1152	0	0	−640	0	0	−896	0	0	−1152	0	0	1152	0	0
ς_{29}	512	0	0	$\frac{896}{3}$	0	0	256	0	0	256	0	0	−896	0	0	0	0	0	0	0	0
ς_{30}	$\frac{640}{3}$	0	0	$-\frac{640}{3}$	0	0	0	0	0	0	0	0	0	0	0	0	0	0	0	0	0
ς_{31}	−4096	0	0	$-\frac{1472}{3}$	0	0	0	0	−256	1536	0	0	9408	0	0	0	0	384	−6912	0	0
ς_{32}	−1024	0	0	$-\frac{704}{3}$	0	0	0	0	384	−128	0	0	2240	0	0	0	0	0	−1152	0	0
ς_{33}	−256	0	0	$\frac{64}{3}$	0	0	0	0	0	−640	0	0	448	0	0	0	0	0	0	0	0
ς_{34}	−64	0	0	$\frac{832}{3}$	0	0	0	0	0	0	0	0	0	0	0	0	0	0	0	0	0
ς_{35}	0	0	256	−256	0	0	0	0	−2304	2304	0	0	0	0	0	0	0	0	0	0	0
ς_{36}	0	0	0	−256	0	0	0	0	−768	1536	0	0	0	0	0	0	0	0	0	0	0
ς_{37}	0	0	0	−256	0	0	0	0	0	768	0	0	0	0	0	0	0	0	0	0	0
ς_{38}	0	0	0	−256	0	0	0	0	0	0	0	0	0	0	0	0	0	0	0	0	0

Table 8
Values of $\varsigma_i(B_j)$ for $i = 1, \dots, 38$, $j = 40, \dots, 51$, where ς_i is defined in (25), (26), and (27).

	B_{40}	B_{41}	B_{42}	B_{43}	B_{44}	B_{45}	B_{46}	B_{47}	B_{48}	B_{49}	B_{50}	B_{51}
ς_1	0	0	0	0	0	0	0	0	0	0	0	0
ς_2	0	0	0	0	0	0	0	0	0	0	0	0
ς_3	0	0	0	0	0	0	0	0	0	0	0	0
ς_4	0	0	0	0	0	0	0	0	0	0	0	0
ς_5	0	0	0	0	0	0	0	0	0	0	0	0
ς_6	0	0	0	0	0	0	0	0	0	0	0	0
ς_7	0	0	0	0	0	0	0	0	0	0	0	0
ς_8	0	0	0	0	0	0	0	0	0	0	0	0
ς_9	0	0	0	0	0	0	0	0	0	0	0	0
ς_{10}	0	0	0	0	0	0	0	0	0	0	0	0
ς_{11}	0	0	0	0	0	0	0	0	0	0	0	0
ς_{12}	0	0	0	0	0	0	0	0	0	0	0	0
ς_{13}	0	0	0	0	0	0	0	0	0	0	0	0
ς_{14}	0	0	0	0	0	0	0	0	0	0	0	0
ς_{15}	0	0	0	0	0	0	0	0	0	0	0	0
ς_{16}	0	0	0	0	0	0	0	0	0	0	0	0
ς_{17}	0	0	0	0	0	0	0	0	0	0	0	0
ς_{18}	0	0	0	0	0	0	0	0	0	0	0	0
ς_{19}	0	0	0	0	0	0	0	0	0	0	0	0
ς_{20}	0	0	0	0	0	0	0	0	0	0	0	0
ς_{21}	0	0	0	0	0	0	0	0	0	0	0	0
ς_{22}	0	0	0	0	0	0	0	0	0	0	0	0
ς_{23}	768	256	0	0	0	0	0	0	0	0	0	0
ς_{24}	0	0	0	0	0	0	0	0	0	0	0	0
ς_{25}	0	0	0	0	0	0	0	0	0	0	0	0
ς_{26}	0	0	0	0	0	0	0	0	0	0	0	0
ς_{27}	0	0	0	0	0	0	96	0	0	1440	0	0
ς_{28}	0	0	0	0	0	0	0	0	0	0	0	0
ς_{29}	0	0	0	0	0	0	0	0	0	0	0	0
ς_{30}	0	0	0	0	0	0	0	0	0	0	0	0
ς_{31}	0	0	256	768	0	0	0	0	0	0	0	0
ς_{32}	0	0	0	0	0	0	0	0	0	0	0	0
ς_{33}	0	0	0	0	0	0	0	0	0	0	0	0
ς_{34}	0	0	0	0	0	0	0	0	0	0	0	0
ς_{35}	0	0	0	0	0	0	0	0	0	0	0	0
ς_{36}	0	0	0	0	0	0	0	0	0	0	0	0
ς_{37}	0	0	0	0	0	0	0	0	0	0	0	0
ς_{38}	0	0	0	0	0	0	0	0	0	0	0	0

[10] J. Grošelj, H. Speleers, Construction and analysis of cubic Powell–Sabin B-splines, Comput. Aided Geom. Des. 57 (2017) 1–22.
[11] J. Grošelj, H. Speleers, Super-smooth cubic Powell–Sabin splines on three-directional triangulations: B-spline representation and subdivision, J. Comput. Appl. Math. 386 (2021) 113245.
[12] M.-J. Lai, Geometric interpretation of smoothness conditions of triangular polynomial patches, Comput. Aided Geom. Des. 14 (1997) 191–199.
[13] M.-J. Lai, L.L. Schumaker, Spline Functions on Triangulations, Encyclopedia of Mathematics and Its Applications, vol. 110, Cambridge University Press, Cambridge, 2007.
[14] T. Lyche, C. Manni, H. Speleers, Foundations of spline theory: B-splines, spline approximation, and hierarchical refinement, in: T. Lyche, et al. (Eds.), Splines and PDEs: From Approximation Theory to Numerical Linear Algebra, in: Lecture Notes in Mathematics, vol. 2219, Springer, 2018, pp. 1–76.
[15] T. Lyche, C. Manni, H. Speleers, Construction of C^2 cubic splines on arbitrary triangulations, Found. Comput. Math. 22 (2022) 1309–1350.
[16] T. Lyche, J.-L. Merrien, Simplex-splines on the Clough–Tocher element, Comput. Aided Geom. Des. 65 (2018) 76–92.
[17] T. Lyche, J.-L. Merrien, A C^1 simplex-spline basis for the Alfeld split in $\mathbb{R}^s$, preprint, 2022.
[18] T. Lyche, J.-L. Merrien, T. Sauer, Simplex-splines on the Clough–Tocher split with arbitrary smoothness, in: C. Manni, H. Speleers (Eds.), Geometric Challenges in Isogeometric Analysis, in: Springer INdAM Series, vol. 49, Springer, 2022, pp. 85–121.
[19] T. Lyche, G. Muntingh, Stable simplex spline bases for C^3 quintics on the Powell–Sabin 12-split, Constr. Approx. 45 (2017) 1–32.
[20] C.A. Micchelli, On a numerically efficient method for computing multivariate B-splines, in: W. Schempp, K. Zeller (Eds.), Multivariate Approximation Theory, in: Internat. Ser. Numer. Math., vol. 51, Birkhäuser, Basel–Boston, 1979, pp. 211–248.
[21] M.J.D. Powell, M.A. Sabin, Piecewise quadratic approximations on triangles, ACM Trans. Math. Softw. 3 (1977) 316–325.
[22] H. Prautzsch, W. Boehm, M. Paluszny, Bézier and B-Spline Techniques, Mathematics and Visualization, Springer–Verlag, Berlin, 2002.
[23] P. Sablonnière, Composite finite elements of class C^k, J. Comput. Appl. Math. 12–13 (1985) 541–550.
[24] L.L. Schumaker, Spline Functions: Basic Theory, 3rd edition, Cambridge University Press, Cambridge, 2007.
[25] L.L. Schumaker, T. Sorokina, Smooth macro-elements on Powell–Sabin-12 splits, Math. Comput. 75 (2006) 711–726.
[26] H.-P. Seidel, Polar forms and triangular B-spline surfaces, in: Blossoming: The New Polar Form Approach to Spline Curves and Surfaces, Siggraph'91, in: Course Notes, vol. 26, World Scientific Publishing Company, 1992, pp. 235–286.
[27] H. Speleers, A normalized basis for quintic Powell–Sabin splines, Comput. Aided Geom. Des. 27 (2010) 438–457.
[28] H. Speleers, A normalized basis for reduced Clough–Tocher splines, Comput. Aided Geom. Des. 27 (2010) 700–712.
[29] H. Speleers, Construction of normalized B-splines for a family of smooth spline spaces over Powell–Sabin triangulations, Constr. Approx. 37 (2013) 41–72.
[30] H. Speleers, A new B-spline representation for cubic splines over Powell–Sabin triangulations, Comput. Aided Geom. Des. 37 (2015) 42–56.
[31] R.-H. Wang, Multivariate Spline Functions and Their Applications, Kluwer Academic Publishers, Beijing, 2001.
[32] R.-H. Wang, X.-Q. Shi, $S^{\mu}_{\mu+1}$ surface interpolations over triangulations, in: A.G. Law, C.L. Wang (Eds.), Approximation, Optimization and Computing: Theory and Applications, Elsevier Science Publishers B.V., 1990, pp. 205–208.
[33] A. Ženíšek, A general theorem on triangular finite $C^{(m)}$-elements, Rev. Fr. Autom. Inform. Rech. Opér., Sér. Rouge 8 (1974) 119–127.